Title: Observations of radiation belt losses due to cyclotron wave-particle interactions

Abstract

Electron loss to the atmosphere plays a critical role in driving dynamics of the Earth's Van Allen radiation belts and slot region. This is a review of atmospheric loss of radiation belt electrons caused by plasma wave scattering via Doppler-shifted cyclotron resonance. In particular, the focus is on observational signatures of electron loss, which include direct measurements of precipitating electrons, measured properties of waves that drive precipitation, and variations in the trapped population resulting from loss. We discuss wave and precipitation measurements from recent missions, including simultaneous multi-payload observations, which have provided new insight into the dynamic nature of the radiation belts.

Introduction

The Van Allen radiation belts are toruses of semi-trapped, high-energy electrons and ions surrounding the Earth *[e.g. Van Allen, 1959]*. Typical belt structure consists of an inner zone of stably-trapped energetic ions and electrons, and a dynamic outer zone of energetic electrons. These are often separated by a slot region devoid of energetic particles. Storm-time dynamics of the radiation belts arise from competition of a number of time-varying processes that enhance or deplete energetic electron populations. These include energization or de-energization from radial transport [*Li et al., 1997*; *Shprits et al., 2006*], outer boundary loss [*Turner et al., 2012*; *Hudson et al., 2014*; *Ukhorskiy et al., 2015*], dramatic local acceleration events [*Horne et al., 2005*; *Thorne et al., 2013*; *Matsui et al., 2017*], and steady or bursty precipitation loss to the atmosphere [*Thorne et al., 2010*; *Millan et al., 2011*]. The complex interplay of these processes, driven by a dynamic solar wind [*Hudson et al., 2008*; *Reeves et al., 2011*; *Li et al., 2015c; Boynton et al., 2017*] and influenced by pre-storm magnetospheric conditions [*Kilpua et al., 2015*], ultimately leaves the radiation belts enhanced, depleted, or relatively unchanged over pre-storm levels. [*Friedel et al., 2002*; *Reeves et al., 2003*; *Turner et al., 2015*; *Moya et al., 2017*]

Understanding the relative importance, time-variability, and interrelationships of these drivers is required for predicting short- and long-term space weather. Enhanced predictive capability [*Baker et al., 2012*; *Meredith et al., 2017*] provides the foundation for mitigation strategies protecting satellites against accumulated radiation dose or single event damage [*Wrenn and Smith, 1996*; *Horne et al., 2013a*], enhancements in GPS accuracy, and understanding the effects of space weather on climate via modification of upper atmosphere chemistry [*Miranova et al., 2015*] including ozone depletion *[Andersson et al., 2014]*.

This review focuses on one aspect of this complex system; loss of energetic (>~100 keV), relativistic (>500 keV) and ultra-relativistic (>2 MeV) electrons to the atmosphere through

Doppler-shifted cyclotron resonance with waves. In particular, the focus is on observational signatures of electron precipitation and comparison with measured properties of the plasma waves that drive a substantial part of this loss. Section 1 reviews the basics of Doppler-shifted cyclotron resonance scattering of electrons by plasma waves, along with quasi-linear theory, which is the dominant paradigm for describing the collective effects of scattering. We provide a brief overview of the various types of energetic electron precipitation observed, followed by a review of the three waves most responsible for causing radiation belt precipitation loss: plasmaspheric hiss, chorus, and electromagnetic ion cyclotron (EMIC) waves. Section 2 then discusses the structure and dynamics of the radiation belts, and in particular the role cyclotron resonance scattering via these three waves plays in dictating belt morphology. Section 3 presents recent single-satellite observations of wave properties, and simultaneous, multi-payload comparative observations of waves and precipitation. These observations provide further insight into resonant scattering and allow close comparison of waves and precipitation loss, necessary for testing models. We conclude this review by discussing important current issues being explored, new approaches to radiation belt understanding (modeling), and the usage of new techniques that promise to enhance our understanding of precipitation loss via Doppler-shifted cyclotron resonant scattering.

1: Background:
1.1 Doppler-shifted cyclotron resonance and quasi-linear theory

Magnetospheric electrons have helical trajectories that are a combination of cyclotron motion about the magnetic field and translation along the field line. The vector sum of these motions describes a cone of velocity vectors with a *pitch angle* relative to the magnetic field. In the magnetosphere, these electrons exist in a magnetic bottle configuration. As electrons propagate to higher magnetic latitudes, magnetic field line convergence produces an effective *mirror* force opposing the electron motion. For electrons with pitch angles outside of the *loss cone*, this force is sufficient to reverse the guiding center motion, sending the electrons back towards the opposite hemisphere and effectively trapping them inside the magnetic bottle. Electrons with pitch angles inside the loss cone, however, have sufficient velocity parallel to the background field to overcome this mirror force, and will precipitate into the atmosphere. Due to the azimuthally asymmetric nature of the Earth's magnetic field, the size of the loss cone varies with geographic longitude and hemisphere. Particles scattered into the *bounce loss cone* (BLC) will precipitate within a single bounce period, while particles scattered into the larger *drift loss cone* (DLC) will precipitate within one drift period once they reach a region of weaker magnetic field called the *South Atlantic Anomaly*.

Electrons trapped in the magnetic bottle geometry can be scattered into the loss cone by interaction with circularly/elliptically polarized waves in a process called Doppler-shifted cyclotron resonance *[e.g. Tsurutani and Lakhina, 1997]. Normal* resonance occurs between a counter-streaming electron with field-aligned velocity $v_\parallel$, and right-hand polarized wave, with field-aligned wave number $k_\parallel$ and angular frequency $\omega < \omega_{ce}$, where ω_{ce} is the cyclotron frequency. Resonant electrons observe the wave Doppler-shifted to an integral multiple n (n=0, +/-1, +/-2, ...) of their cyclotron frequency, satisfying the resonance condition:
$$\omega - k_\parallel v_\parallel = n\Omega_{ce}/\gamma, \qquad\qquad (1)$$
where γ is the relativistic Lorentz factor. *Anomalous* resonance [*Ginzburg, 1960*] can occur between a co-propagating electron and left-hand polarized wave if the electron velocity exceeds

the wave phase velocity. In the frame of the electron this shifts the sense of wave rotation from left to right, allowing resonance to occur. Anomalous resonance allows left-hand polarized waves, such as EMIC waves, to interact with highly energetic (typically multi-MeV) electrons. Electrons in resonance (either normal or anomalous) see a constant wave phase and are able to efficiently exchange energy and momentum with the wave *[Brice, 1964]*.

To determine the importance of Doppler-shifted cyclotron resonance interactions in magnetospheric dynamics we're seldom interested in the details of any single wave/electron interaction. In the quasi-linear paradigm, the combined effect of a number of weak scattering interactions involving small amplitude, broadband waves and a phase-randomized distribution of electrons results in diffusion of electrons in pitch angle and energy *[Kennel and Petschek, 1966; Kennel and Engelmann, 1966]*. For decades, quasi-linear theory, due to its relative simplicity and utility, has been an important foundation for modeling and understanding radiation belt dynamics (see review by *Horne et al., 2016*). Modern quasi-linear simulations, utilizing the most up to date wave statistical parameterizations and plasma models constructed from decades of satellite observations, have found success describing long-duration (days to weeks) evolution of radiation belt populations [e.g. *Subbotin et al., 2011; Kim et al., 2013; Tu et al., 2013; Shprits et al., 2009*].

A simple metric calculated from quasi-linear theory for describing the integrated effect of multiple source and loss processes is the *electron lifetime*, defined as the e-folding loss timescale for electrons [e.g. *Shprits et al., 2007*; *Albert and Shprits, 2009*]. In the Earth's radiation belts, electron lifetimes are driven largely by Doppler-shifted cyclotron resonance scattering with three prominent plasma waves: plasmaspheric hiss, chorus, and EMIC. These are discussed in detail in Section 1.3. Loss by these waves plays an important role in creating the classic two-belt structure of the Earth's radiation belts.
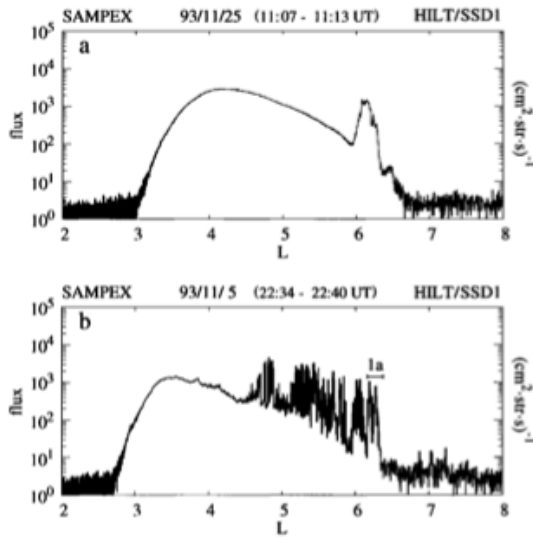
1.2 Overview of precipitation observations

A long history of observations has established that precipitation into the atmosphere is an important source of radiation belt electron loss. Precipitation is observed to come in a variety of forms ranging from slow drizzle to impulsive, subsecond events. Tying the various forms of precipitation to potential causative waves, typically observed near the equator, is critical for understanding this connection. This comparison turns out to be exceedingly difficult in practice. Equatorial satellites are ideally suited for measuring in situ wave populations generated near the magnetic equator, but are often unable to distinguish between trapped and precipitating electrons. High inclination, low Earth orbit (LEO) satellites can directly observe precipitating electrons but are usually far from the wave source. More continuous, albeit indirect precipitation observations come from balloons, which infer precipitating spectra from measurements of X-rays produced by bremsstrahlung interaction with atmospheric neutrals [*Woodger et al., 2015*; *Millan et al., 2013*; *Foat et al., 1998*], as well as from ground-based platforms like riometers and VLF receivers, which indirectly measure precipitation through its effect on atmospheric ionization [e.g. *Rodger et al., 2012; Clilverd et al., 2009*]. Due to accessibility and low relative cost, balloons and ground-based platforms provided the majority of precipitation observations in the early decades of radiation belt research [e.g. *Rosenberg et al., 1971*].

LEO spacecraft, due to their fast traversal of the radiation belts, provide a snapshot of electron precipitating populations at a given time interval. Figure 1, adapted from *Nakamura et al.* [2000], shows two example passes through the outer radiation belt of >1 MeV electron flux

measured by the LEO satellite SAMPEX. Figure 1a shows a well-populated outer belt from L~3-7 superimposed with a relativistic electron precipitation (REP) band of strongly enhanced flux at L~6. These bands are often seen on consecutive orbits and/or in conjugate hemispheres. The observed repeatability and duration is thought to reflect a persistent (lasting minutes to hours), latitudinally narrow precipitation region [*Nakamura et al., 1995*; *Blake et al., 1996*]. Balloon and satellite observations show that REP events occur predominantly in the afternoon and night sectors, with increased frequency during geomagnetic activity [*Millan et al., 2002*; *Imhof et al., 1986*; *Nakamura et al., 2000*; *Comess et al., 2013*; *Blum et al., 2015a*]. Numerous studies attempting to identify the causes of these precipitation events have categorized them into different groups based on shape, duration, and whether simultaneous lower energy electron or ion precipitation is observed [e.g. *Yahnin et al., 2016*; *Vampola 1971*, *Imhof et al., 1986*]. Some of these precipitation events have been attributed to a breakdown of adiabaticity in the warped nightside magnetic field geometry, while others have been attributed to scattering by various wave modes [*Vampola 1971*; *Koons et al., 1972*; *Brown and Stone 1972*]. They have been estimated to be an important source of >MeV electron loss, particularly during geomagnetically active periods [*Bortnik et al., 2006*; *Millan et al., 2002*; *Blum et al., 2013*].

Figure 1b shows an example of a well-populated outer zone superimposed with short-duration spikes of high precipitation flux. These spikes, occurring on subsecond timescales, are termed microbursts. Microbursts were initially observed at ~keV energies [*Winckler et al., 1962*; *Anderson and Milton 1964*, *Tsurutani et al., 2013*, *Lampton 1967*], and more recently at relativistic (MeV) energies [*Imhof et al., 1992*; *Blake et al., 1996*; *Crew et al., 2016*]. Microbursts are most common during storm main and early recovery phases [*O'Brien et al., 2004*], are typically found in the morning sector and outside of the plasmasphere [*Lorentzen et al., 2001a, b; Johnston and Anderson, 2010*; *Douma et al., 2017*], and often occur in long trains (e.g. Figure 1b). These observations have led to suggestions that they are caused by impulsive, nonlinear scattering [e.g. *Blake et al., 1996*; *Hikishima et al., 2010*; *Osmane et al., 2016*]. Comparisons of precipitating microburst flux to trapped population estimates are subject to large uncertainties, but indicate that long-lasting and extended sources of relativistic microbursts [*Anderson et al., 2017*] can be a major source of electron loss during storm times [*Lorentzen et al., 2001b*; *O'Brien et al., 2004*; *Breneman et al., 2017*].

Figure 1 (Adapted from *Nakamura et al., 2000*): SAMPEX observations of >1 MeV electron flux from two passes through the outer radiation belts, with (a) showing smoothly varying flux with a well-defined precipitation band, and (b) showing strong flux contributions from relativistic microbursts.

SAMPEX   93/11/25 (11:07 - 11:13 UT)   HILT/SSD1

a

flux

10^5
10^4
10^3
10^2
10^1
10^0

(cm^2-str-s)$^{-1}$

2   3   4   5   6   7   8
L

SAMPEX   93/11/ 5 (22:34 - 22:40 UT)   HILT/SSD1

b

flux

10^5
10^4
10^3
10^2
10^1
10^0

1a

(cm^2-str-s)$^{-1}$

2   3   4   5   6   7   8
L

Despite decades of observations, large gaps remain in our understanding of energetic, relativistic, and ultra-relativistic electron precipitation. It is yet unclear what fraction of precipitation loss results from wave resonance scattering as opposed to other mechanisms such as breakdown of adiabaticity in the tail region. Also unclear is how the theoretical energy dependence of scattering by various wave modes matches up with observations. Finally, there is an incomplete understanding of the relative importance of precipitation loss compared to other loss mechanisms, such as outer boundary loss. To complicate matters, the relative importance of wave-induced loss, as well as the details of this loss, can be highly variable within the evolution of a single storm, and from storm to storm. The remainder of this review aims to address the role that different wave modes play in causing electron precipitation, and the overall contribution of this precipitation to the dynamics of the Earth's radiation belts.

1.3 Key wave modes involved in radiation belt electron loss

We now provide a brief overview of plasmaspheric hiss, chorus, and EMIC waves. These wave types are thought to dominate resonant scattering loss of radiation belt electrons. Other wave types, such as VLF transmitters, lightning whistlers, magnetosonic waves, and kinetic Alfven waves, play small or supporting roles in scattering loss [*Abel and Thorne, 1998*] and are not extensively discussed here.

Figure 2: Magnetic field power spectral density during periods of (a) unstructured plasmaspheric hiss, (b) lower and upper band chorus tones, and (c) electromagnetic ion cyclotron (EMIC) wave activity.

(a) Hiss

(b) Chorus

(c) EMIC

20 June 2013 UTC
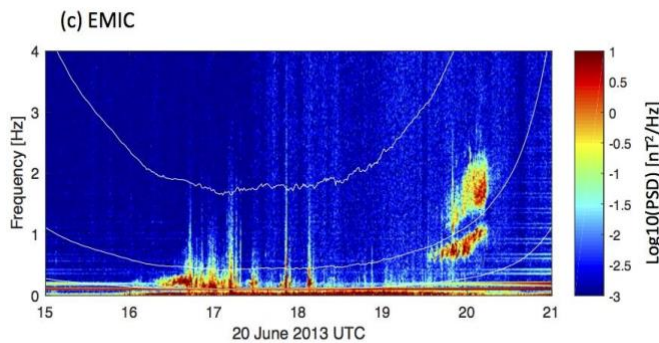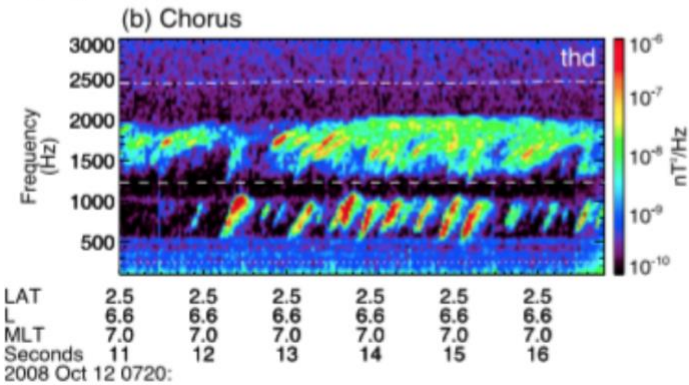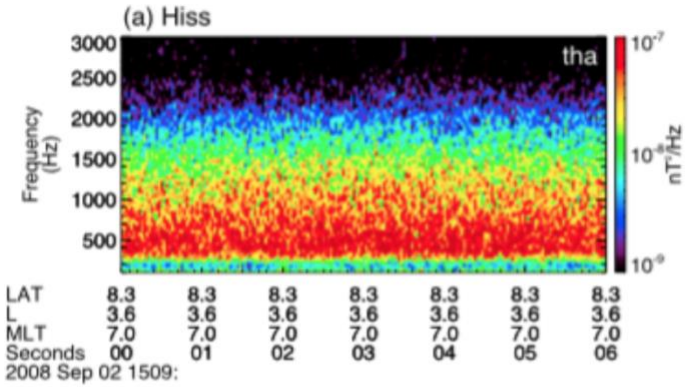
1.3.1 Plasmaspheric Hiss

Plasmaspheric hiss [*Thorne et al., 1973*] is a typically structureless, broadband electromagnetic whistler mode emission (Figure 2a) found within the high density plasmasphere and plasmaspheric plumes. Wave amplitudes usually range from 10-100 pT and peak at ~300-400 Hz [*Meredith et al., 2004*; *Golden et al., 2012*; *Yu et al., 2017*; *Li et al., 2015b*]. Various other types of hiss have been observed, such as mid-latitude hiss (see review by *Hayakawa and Sazhin, 1992*), dayside hiss following shock compressions [*Tsurutani et al., 2015*], low altitude or ionospheric hiss [*Chen et al., 2017*; *Zhima et al., 2017*], and plasma trough exohiss [*Zhu et al., 2015*], but the focus in this review is on the more dynamically important plasmaspheric hiss.

Despite being one of the most ubiquitous plasma waves, the processes leading to hiss growth have been difficult to pin down. Early theories (e.g. *Thorne et al., 1973*) suggested local growth near the magnetic equator via temperature anisotropy instability, but this idea was later

rejected as offering insufficient growth [*Huang et al., 1983*; *Church and Thorne, 1983*]. Recent Poynting flux observations from the Van Allen Probes, however, indicate in situ generation near the magnetic equator for at least some fraction of plamaspheric hiss [*Kletzing et al., 2014 AGU abstract*]. Local generation can also occur within radial extensions of the plasmasphere called plumes [*Laakso et al., 2015*]. Hiss that does not grow locally appears to originate with whistler mode chorus that has propagated into the plasmasphere after reflection at low altitudes [*Parrot et al., 2004; Chum et al., 2005; Santolik et al., 2006; Bortnik et al., 2008*; *Bortnik et al., 2009*; *Santolik et al., 2009; Yue et al., 2017; Hartley et al., 2018*]. Once inside, damping rates are significantly reduced [*Li et al., 2010*] allowing these waves to propagate long distances and mix to form a hiss-like spectrum. This direct connection between chorus and hiss has been verified observationally [*Li et al., 2015a*; *Bortnik et al., 2011*; *Chen et al., 2012*; *Delport et al., 2012*; *Meredith et al., 2013*; *Zhou et al., 2016*], and with ray tracing invoking modest in situ growth [*Bortnik et al., 2011*; *Chen et al., 2012*; *Thorne et al., 1979*; *Tsurutani et al., 2012*].

Hiss waves can interact via cyclotron resonance with a wide range of electron energies, from few keV to MeV, and scattering by hiss waves within the plasmasphere is recognized to play a dominant role in creating the quiet-time structure of the slot region and radiation belts [*Lyons et al., 1972*; *He et al., 2016*].

1.3.2 Chorus

Whistler mode chorus is a prominent VLF wave that exists in the low density magnetosphere outside of the plasmasphere [*Burtis and Helliwell, 1969*; *Tsurutani and Smith, 1974; Sazhin and Hayakawa, 1992*]. Chorus waves (Figure 2b) are often observed as distinctive rising or (less frequently) falling tones of several kHz/sec [*Santolik et al., 2004*; *Macusova et al., 2010*]. Wave power is separated into a lower band (~0.1-0.5 f_{ce0}, where f_{ce0} is the minimum electron cyclotron frequency along a particular field line) and an upper band (0.5-0.8 f_{ce0}), often with a gap at 0.5 f_{ce0} [*Tsurutani and Smith, 1977*; *Santolik et al., 2005*]. Lower band chorus is typically much stronger and more common than upper band chorus [*W. Li et al., 2012*], and interacts with higher energy electrons.

Chorus grows near the magnetic equator [*Nagano et al., 1996*; *LeDocq et al., 1998*; *Parrot et al., 2003; Santolik et al., 2005*] around midnight in association with injections of few keV to tens of keV plasma sheet electrons during substorm onset [*Tsurutani and Smith, 1974*; *Xiao et al.*, *1998*; *Meredith et al., 2001*; *Li et al.*, *2009*; *Summers et al.*, *2009*; *Jordanova et al.*, *2010*; *Yue et al., 2017*], on the dawn side in association with enhanced convection that can occur pre-substorm or during the substorm growth phase [*Hwang et al., 2007*], and in higher latitude minimum magnetic field pockets formed during times of enhanced dayside compression [*Spasojevic and Inan, 2010; Tsurutani and Smith, 1977*; *Meredith et al., 2001*]. In all these cases, initial wave growth arises from the temperature anisotropy instability [*Kennel and Petschek, 1966*; *Omura and Summers, 2004*; *Summers et al., 2009*; *Fu et al., 2014*; *Yue et al., 2016*], and results in electron scattering to lower pitch angles [*Brice, 1964*], leading to precipitation in the form of few keV diffuse aurora [*Thorne et al., 2010*], tens of keV pulsating aurora [*Nishimura et al., 2010*], and microbursts [*Oliven and Gurnett, 1968; Rosenberg et al., 1981*]. Once amplitudes grow beyond a critical threshold, nonlinear phase bunching and trapping occur [*Nunn 1974*; *Omura and Summers, 2006*; *Katoh and Omura, 2007*; *Shkylar and Matsumoto, 2009*; *Omura et al., 2012*; *Matsui et al., 2016*], and facilitated by magnetic field

inhomogeneity, this can lead to the classic chirping, narrowband tones [*Katoh et al., 2013*; *Teng et al., 2017*], and allows energy and momentum exchange with resonant electrons.

For hundreds of keV electrons, chorus waves are both theorized [*Summers et al., 1998*, *Horne and Thorne, 1998*; *Roth et al., 1999*; *Horne et al., 2003a, b*; *Horne et al., 2005*] and observed [*Meredith et al., 2002*; *Meredith et al., 2003a*; *Chen et al., 2007*; *Xiao et al., 2014*; *Su et al., 2014*; *Jaynes et al., 2015*; *Rodger et al., 2016*; *Foster et al., 2017*] to play a dual role [*Bortnik et al., 2007; Millan and Baker, 2012*] of driving both dramatic, localized storm-time enhancements of electrons to MeV energies, and causing significant electron precipitation loss up to MeV energies, including microbursts [*Agapitov et al., 2018*; *Lorentzen et al., 2001a*].

1.3.3 EMIC

Electromagnetic ion cyclotron (EMIC) waves are electromagnetic fluctuations that occur at frequencies below and approaching the local ion (H+, He+, O+) cyclotron frequencies, around 0.1-5 Hz in the heart of the outer radiation belt (see Figure 2c). Occurrence rates peak across the dayside and afternoon sectors [e.g. *Saikin et al., 2015*; *Wang et al., 2015*], with He+ band waves often more prevalent and of larger amplitude in the dusk sector, while H+ band waves are more often located in the day and morning sectors [e.g. *Min et al., 2012*; *Keika et al., 2013*]. A recent study of O+ band waves, less often surveyed than H+ and He+, found these waves to be prevalent in morning and noon sector as well [*Yu et al., 2015*].

EMIC waves are thought to be generated from keV ion populations with an unstable temperature anisotropy ($T_\perp > T_\parallel$) [*Cornwall et al., 1965*; *Horne and Thorne, 1994*]. The presence of cold plasma lowers the instability threshold, enabling enhanced wave growth [e.g. *Gary 1993*]. In the inner magnetosphere, EMIC waves often occur in the afternoon sector where keV ring current ions overlap cool, dense plasmaspheric plumes [e.g. *Spasojevic et al., 2005*; *Clausen et al., 2011*; *Halford et al., 2010*]. EMIC waves can also be generated across the dayside during times of enhanced solar wind dynamic pressure, which acts as a source of temperature anisotropy as well [*McCollough et al., 2010*; *Usanova et al., 2012*]. Ray tracing models have suggested that density gradients, found at the plasmapause and in fine structure of plasmaspheric plumes, can support enhanced EMIC wave growth [*Chen et al., 2009*; *de Soria SantaCruz et al., 2013*]. However, observationally, EMIC wave dependence on cold plasma structures is less clear, with some studies finding a relationship between EMIC occurrence and enhanced cold plasma density and/or density gradients [e.g. *Halford et al., 2015*], and others finding little statistical correspondence [e.g. *Usanova et al., 2013*; *Posch et al., 2010*; *Fraser and Nguyen, 2001*].

EMIC waves have long been theorized to precipitate radiation belt electrons through anomalous cyclotron resonance [*Thorne and Kennel, 1971*]. The energy of electrons resonant with EMIC waves, based on observed plasma and wave parameters, typically falls in the multi-MeV range [*Meredith et al., 2003b*; *Loto'aniu et al., 2005*; *Ni et al., 2017*], but can be lowered with increased cold plasma density [*Li et al., 2013*], or as the wave frequency approaches a heavy ion cyclotron frequency [*Ukhorskiy et al., 2010*]. EMIC waves can also resonate with and scatter keV ions, acting as a loss process for the ring current [*Cornwall et al., 1970*; *Jordanova et al., 2007*]. For this reason, simultaneous keV ion and MeV electron precipitation is often interpreted as a signature of EMIC wave scattering [e.g. *Sandanger et al., 2007*; *Miyoshi et al., 2008*; *Carson et al., 2013*]. Theoretical estimates have shown that EMIC waves can produce scattering near the strong diffusion limit and thus may contribute to rapid losses of outer belt electrons [e.g. *Summers and Thorne, 2003*]. However, warm plasma, nonlinear, and non-

resonant effects can all complicate these interactions, leading potentially to increased minimum resonant energies, reduction in scattering rates, or scattering into the loss cone at non-resonant energies [e.g. *Chen et al., 2011; Silin et al., 2011; Albert and Bortnik, 2009; Chen et al., 2016*], to be discussed in more detail in Section 3.

2: Radiation belt structure and morphology

Figure 3 (from *Reeves et al., 2016*): Electron flux levels as a function of L-shell and energy from Van Allen Probes measurements showing (a) the nominal quiet-time structure with clear separation between inner zone, slot, and outer belt regions across a wide range of energies, and (b) belt structure following active time enhancements showing a much less distinct separation between the three zones.
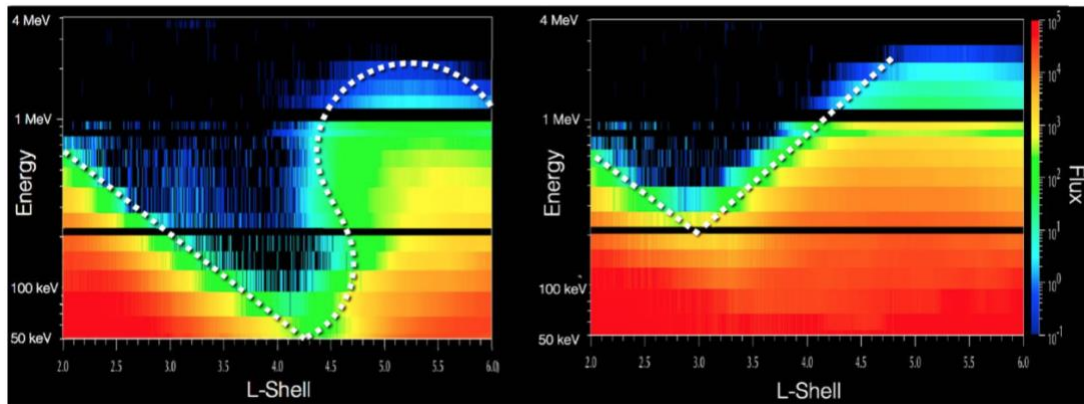

The classic quiet-time structure of the radiation belts consists of two toruses of energetic particles surrounding the Earth - a relatively static inner zone of energetic ions and electrons, and a more dynamic outer zone of energetic electrons. These are separated by a slot region largely devoid of energetic electrons. What is often not depicted in this classic picture is the strong energy, L shell, and geomagnetic activity dependence of these fluxes and zone boundaries, as illustrated in the Van Allen Probes observations of Figure 3 [*Reeves et al., 2016*]. Radiation belt structure during quiet-times (3a) and following active time enhancements (3b) is distinctly different. This structure is formed as a balance of different acceleration and loss processes that vary in relative importance with storm phase. The efficiency of each process depends on electron energy, wave frequency, and location, with important differences occurring inside and outside of the plasmapause.

Quiet time morphology shows a distinct separation between inner and outer zones. This zonal separation diminishes during active times where enhanced radial transport [*Brautigam and Albert, 2000; Zhao and Li, 2013b*] and local energization processes [e.g. *Baker et al., 2014*; *Ma et al., 2017*] enhance flux levels, partially or fully filling the slot region. These enhancements temporarily overwhelm loss processes which include outward radial diffusion, outer boundary loss at the magnetopause, and precipitation loss. As the driving geomagnetic activity subsides, transport and energization processes begin to lose out to wave-induced precipitation loss, and the radiation belts gradually return to the quiet-time configuration in Figure 3a.

We now discuss details of how this balance leads to both the quiescent and dynamic structure of the radiation belts, focusing on the important role of cyclotron resonant scattering loss caused by plasmaspheric hiss, chorus, and EMIC waves.

2.1 Inner zone and slot

Figure 4 (from *Abel and Thorne, 1998*): Typical minimum resonant cyclotron energies vs L-shell for a range of wave frequencies corresponding to plasmaspheric hiss (~550 Hz), lightning-generated whistlers (4.5 kHz), and VLF transmitters (17.1 and 22.3 kHz).
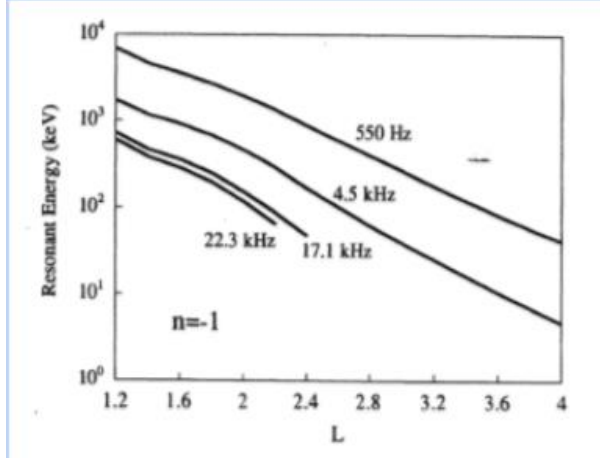
The inner zone is a region of stably trapped ions and energetic electrons, where lifetimes can vary from months to years [e.g. *Hess 1963*; *Walt 1994*]. Lifetimes drop sharply to days to weeks in the adjacent slot region. This sharp transition forms from the combined L-dependence of wave-induced precipitation rates and efficiency of radial transport [*Lyons et al., 1972*; *Lyons and Thorne, 1973*; *Kim et al., 2011*; *He et al., 2016*]. Precipitation rates are dependent on resonance access, meaning that local particles must exceed the minimum cyclotron resonance energy, plotted in Figure 4 vs L for a range of frequencies. Resonance energy increases with decreasing L, due to the increase in background magnetic field strength, and decreases with wave frequency. Electrons with energies below (or well above) this minimum cyclotron energy are unable to effectively resonate with the waves. Near the boundary of the inner zone and slot this minimum resonance energy begins to exceed available electron populations and lifetimes drastically increase.

Electrons are supplied into the slot and inner zone by injections or inward radial transport by ULF waves. Transport rates strongly decrease with increasing energy and decreasing L-shell. Low energy (<100 keV) electron injections, which can occur multiple times per day [*Zhao et al., 2013; Turner et al., 2017*], are able to penetrate further in than higher energy electrons because they have relatively high radial transport rates and their energies are below the minimum cyclotron resonant energy for plasmaspheric hiss. At a given L, as energy increases, injections become less frequent, and electron energies can exceed the minimum cyclotron resonance energy for plasmaspheric hiss, tipping the balance between inward transport and loss gradually towards loss. This results in a widening of the slot region with energy.

At ultra-relativistic (few MeV) energies, radial transport rates are so low [e.g. *Ma et al., 2017a, Fig4*; *O'Brien et al., 2016*; *Zhao et al., 2013*] that wave scattering rates, despite being low, dominate radial transport, creating a sharp inner boundary near L=2.8 termed the

impenetrable barrier [*Baker et al., 2014b*; *Foster et al., 2016*]. This barrier is not absolute, and relativistic electron incursions into the inner belt do occasionally happen during rare and very powerful storms [*Blake et al., 1992*; *X. Li et al., 1993*; *Baker et al., 2004*], though no >1.5 MeV electrons have been observed in the inner zone as of yet during the Van Allen Probes era (2012-2017) due to historically low recorded solar activity [*Claudepierre et al., 2017; Fennell et al., 2015; X. Li et al., 2015*].

This simple picture of a balance of radial transport and plasmaspheric hiss scattering fairly accurately describes the global structure and long term (days) evolution of the inner belt and slot region during storm recovery. Not included, but also important are contributions to scattering loss due to higher frequency (1-2 kHz) lightning-generated *whistlers* [*Storey, 1953*; *Helliwell, 1965*; *Sonwalker and Inan, 1989*; *Abel et al., 2098*; *Meredith et al., 2006a*; *Agapitov et al., 2014*; *Rodger et al., 2003*; *Meredith et al., 2009*; *Kim et al., 2011*], and (10-40 kHz) whistler mode VLF transmitters [*Inan et al., 2007*; *Ma et al., 2017b*]. Though generally containing far less spectral power than plasmaspheric hiss, the higher frequencies of these waves allow them to scatter electrons with energies below the range in resonance with plasmaspheric hiss.

2.2 Outer Zone

Beyond the previously-discussed inner zone and slot region lies the far more dynamic outer zone [*Paulikas and Blake, 1979*]. Precipitation loss via cyclotron resonance with plasmaspheric hiss, chorus, and EMIC waves plays a large role in its structure and variability. Both steady, longer term decay of the outer radiation belt (e.g. due to scattering by plasmaspheric hiss) as well as more dynamic changes in the population from faster timescale scattering processes, including precipitation loss from EMIC and chorus waves, are observed.

The location of the plasmapause, and waves contained inside this higher density region versus those in the low density region beyond, plays an important role in the structure and evolution of the outer radiation belt. Inside the plasmasphere, plasmaspheric hiss is largely responsible for gradual depletion of electron flux during the storm recovery and quiet times, as is also the case with inner belt electron decay. Electron lifetimes, derived from observations of precipitation [e.g. *Selesnick et al., 2003*; *Jaynes et al., 2014*], as well as from the decay of trapped outer radiation belt electrons [*Meredith et al., 2006b*; *O'Brien et al., 2014*], show good agreement with expected scattering rates driven by hiss waves. On days to months timescales, the inner edge of the outer radiation belt tracks the plasmapause location very closely, further supporting the relationship between plasmaspheric hiss and electron loss [*X. Li et al., 2006*; *Goldstein et al., 2005*].

Outside the plasmasphere, loss can be more dynamic and highly energy-dependent. Rapid (minutes to hours), electron flux dropouts are commonly observed during storm main phase, often wiping out the entire outer radiation belt. Loss to the magnetopause, facilitated by outward radial transport, has been shown to account for a large portion of these depletions, but additional loss is often needed, particularly at lower L shells [e.g. *Turner et al., 2014*; *Hudson et al., 2014*]. Enhanced precipitation to the atmosphere, associated with EMIC and chorus wave scattering, has been observed during some storm main phases and may contribute to these depletions [*Green et al., 2004*; *Xiang et al., 2017*; *Yu et al., 2015*; *Blum et al., 2015a*; *O'Brien et al., 2004*]. Radial profiles of phase space density (PSD) have been used to infer the primary mechanisms active in radiation belt enhancements and depletions. Decaying peaks in PSD can indicate rapid losses to

the magnetopause from a combination of magnetopause shadowing and outward radial diffusion [*Turner et al., 2012*]. In contrast, local minima in PSD profiles at ultra-relativistic energies, recently observed by *Shprits et al.* [*2017*], suggest a rapid energy-selective loss process in the heart of the outer belt, due potentially to scattering by EMIC waves.

However, due to the multitude of possible time-varying acceleration and loss processes acting in the outer zone, it is often difficult to separate out any single process. To accurately estimate enhancement events one must also account for simultaneous losses. A further layer of complexity comes in the form of warping (or asymmetric configuration) of the plasmasphere, which manifests as plumes, shoulders, etc [*Sandel et al., 2003*]. This can allow energetic electrons access to both high and low density plasma environments during the course of a drift orbit. *Summers et al.* [*2008*] showed that loss due to plasmaspheric hiss scattering in a warped plasmasphere or plume can limit electron energization due to interaction with chorus. In this scenario, an electron may experience cyclotron resonant interactions with both whistler mode and EMIC waves over the course of its drift orbit, and thus the combined scattering effects of multiple wave modes must be taken into account [*Ma et al., 2015*; *Mourenas et al., 2016*; *Zhang et al., 2017*].

An illustrative example of this complexity is the formation and subsequent slow depletion of a temporary third *storage* ring at multi-MeV energies following a September, 2012 geomagnetic storm [*Baker et al., 2013*]. On September 3rd, an interplanetary shock triggered a geomagnetic storm and resulted in the rapid depletion of electron flux at L>3.5. Within this distance, though, a narrow belt of ultra-relativistic electrons remained. As local energization processes then reconstituted the outer belt beyond L=4, this storage ring persisted undisturbed for multiple weeks, showing gradual decay consistent with energy-dependent scattering by plasmaspheric hiss [*Thorne et al., 2013*]. Some studies have suggested scattering from EMIC waves may be important for the formation of this 3-belt structure [*Shprits et al., 2013*], while others emphasize the role of ULF-driven radial transport [*Mann et al., 2016a*]. The plasmapause boundary and its relationship to these more complex, energy-dependent radiation belt structures is less straightforward than the longer term averaged picture described previously [*Darrouzet et al., 2013*; *Goldstein et al., 2016*]. Eventually the storage belt was abruptly destroyed following the passage of another interplanetary shock. Storage rings have since been identified in previous periods [e.g. *Yuan and Zong, 2013*; *Kellerman et al., 2014*], and a better understanding of the role of cyclotron resonance in their formation, stability, and ultimate decay is still needed.

The processes contributing to radiation belt precipitation losses have long been studied, but recent observations have revealed new features of the inner belt, slot region, and outer belt morphology and require renewed investigation into the role of various waves and processes in dictating the structure and dynamics of the radiation belts.

3: MODERN SINGLE- AND MULTI-POINT OBSERVATIONS, AND UPDATING THE CLASSIC PICTURE

Observations of detailed wave properties, brought about by an increasingly large dataset of sophisticated spacecraft observations spanning the inner to outer zone, have provided a new look

at waves that have long been measured in Earth's magnetosphere. In the first half of Section 3, we discuss some of these recently observed wave properties and the effects they may have on our understanding of wave-particle resonant scattering. In the second half, we discuss results from simultaneous multi-payload observations, which allow the separation of temporal and spatial effects, and can provide global context during times of rapidly changing radiation belt dynamics.

3.1 New (single-satellite) observations of wave characteristics

An increasing number of sophisticated satellite observations are revealing new properties of waves that have been studied for decades. These include measurements suggesting extended ranges of frequency and wave normal angle, large amplitudes, and wave/plasma and wave/wave coupling. These properties influence how waves interact with electrons, the energies with which they resonate, and the efficiency of loss cone scattering.

3.1.1: Wave populations at extended frequency ranges

Wave frequency helps to determine the energy of cyclotron resonance. For fixed wave normal angle, plasma parameters, and harmonic number, Equation 1 shows that cyclotron resonant energy increases (decreases) as frequency decreases (increases). Proper measurement of wave spectra is necessary for determining the effective range of resonant energies.

A low frequency (~20-100 Hz) population of plasmaspheric hiss has been recently identified [*Li et al., 2013a*] in association with injections of >100 keV plasma sheet electrons that gradient/curvature drift into an asymmetric plasmasphere [*Shi et al., 2017*]. This is an entirely separate population from the more common >100 Hz hiss discussed in Section 2.3.1 [*Malaspina et al., 2017*]. Ray tracing studies suggest that these low frequency hiss waves repeatedly traverse the equatorial amplification region via cyclical ray paths made possible by the low frequencies and refraction near the plasmapause, leading to path-integrated amplification to observed values [*Chen et al., 2014*]. Electron lifetime models derived from hiss scattering show that few hundred keV electron lifetimes can be shortened by a few orders of magnitude due to this low frequency component [*Ni et al., 2014a*; *Orlova et al., 2016*].

Chorus waves are also occasionally observed to extend below their typical frequency range. *Meredith et al.* [*2014*] observed a low frequency extension of chorus power at higher latitudes where the increasing magnetic field strength results in a relative drop in frequency to f/f_{ce}< 0.1. This frequency range is often not accounted for in chorus spectra included in radiation belt models, but may provide important energization and scattering of 100s keV electrons. Chorus is also occasionally observed at f/f_{ce}<0.1 near the equator. *Cattell et al.* [*2015*] observed drops in chorus frequency to f<0.1f_{ce} in association with storm-time injections of ~100 keV electrons, rather than the 10s keV electrons thought to typically lead to chorus growth. Wave amplitudes are often large, and the low frequencies provide much stronger pitch-angle diffusion for >500 keV than typical chorus [*Gao et al., 2016*; *Xiao et al., 2017*].

Recent Van Allen Probes observations have identified oxygen cyclotron harmonic waves as a common occurrence in the inner magnetosphere during geomagnetic storms [*Usanova et al., 2016*]. While electromagnetic ion cyclotron harmonic waves have been observed previously in the inner magnetosphere and plasma sheet boundary layer [e.g. *Perraut et al., 1982*; *Denton et al., 2010*], these observations have been of predominantly compressional, proton harmonic waves. The recent ion cyclotron harmonic waves investigated by *Usanova et al.,* [*2016*] (distinct

from O+ band EMIC waves) were instead most often at O+ harmonic frequencies propagating close to the background magnetic field, with small wave normal angles. These waves, likely previously assumed to be the same as EMIC waves, have wave power concentrated at the O+ cyclotron frequency and its harmonics, rather than having a stop-band at ion cyclotron frequencies as is typical for EMIC waves [e.g. *Kozyra et al., 1984*]. *Ukhorskiy et al.* [*2010*] showed that as the wave frequency approaches the ion cyclotron frequency, EMIC waves can more efficiently scatter electrons of lower energies. The effects of these ion cyclotron harmonic waves are still to be explored.

3.1.2: Wave populations with a wide range of wave normal angles

In addition to frequency, wave normal angle can determine resonant energy for cyclotron interaction as well as pitch angle diffusion rates. Wave polarization changes with increasing wave normal angle, including the development of an electrostatic component along the wave vector [*Stix, 1992*]. This can significantly modify wave-particle resonance, modify the wave dispersion relation, increase the importance of higher-order harmonic ($|n|>1$) contributions to scattering, and introduce significant *Landau* (n=0) interaction [*e.g. Artemyev et al., 2012b*; *Agapitov et al., 2015*; *Hsieh et al., 2017*]. Due to these complexities, a lack of comprehensive statistics, and difficulty of proper inclusion into models, the overall effect of wave obliquity on precipitation rates is not well understood. However, it is possible oblique waves may contribute significantly to precipitation loss. For example, inclusion of a range of wave normal angles of plasmaspheric hiss is thought to be required [e.g. *Tsurutani et al., 2012*] to explain the wide energy extent of the slot region [*Lyons et al., 2072*; *Meredith et al., 2007*; *Ni et al., 2013*; *Albert et al., 1994*; *Glauert et al., 2014*; *Gao et al., 2015*; *Z. He et al., 2016*; *Ripoll et al., 2017*]. Oblique chorus waves prevalent above about 25° latitude [e.g. *Haque et al., 2010*] may be responsible for creating relativistic microbursts [*Horne et al., 2003b*; *Breneman et al., 2017*].

Near the magnetic equator, a subpopulation of highly oblique, quasi-electrostatic chorus with wave normal angles near the resonance cone is often observed [*Taubenschuss et al., 2014*; *Li et al., 2016*]. Despite carrying only a small fraction of the total wave magnetic energy, these may lead to a significant reduction of electron lifetimes (1-2 orders of magnitude) over a wide range of activity levels [*Artemyev et al., 2012a*; *Mourenas et al., 2012*; *Mourenas et al., 2014*; *W. Li et al., 2014*; *Artemyev et al., 2015*]. Near the loss cone, wave properties are highly sensitive to small variations in wave normal angle, and accurately measuring the maximum index of refraction is critical in determining whether diffusion rates are ultimately higher or lower as compared to field-aligned waves [*Albert et al., 2017*; *Ma et al., 2017c*]. Significant observational and theoretical/modeling work [e.g. *Artemyev et al., 2016, Agapitov et al., 2018a*] remains to properly quantify the role oblique chorus plays in energetic outer belt electron loss.

**3.1.3 Wave element structure/coherence**

Structure and/or coherence in waves can have an important effect on electron scattering. Coherent scattering interactions may result in significantly enhanced rates of pitch angle scattering relative to broadband, unstructured waves [e.g. *Lakhina et al., 2010*; *Bellan et al., 2013*]. The stereotypical example of this is chorus waves, which are often observed to consist of a succession of narrowband, chirping tones [e.g. *Gao et al., 2014*; *Crabtree et al., 2017*; *Santolik et al., 2014a*]. Nonlinear test particle simulations show that discrete chorus packets can lead to

discrete microbursts over a wide range of energies, from 10-100 keV [*Rosenberg et al., 1990*; *Hikishima et al., 2010*] to MeV [*Saito et al., 2012*].

Plasmaspheric hiss, as its name implies, is traditionally characterized as a structureless, broadband emission. This is supported by decades of observations from low resolution satellite spectra (e.g. Figure 2a). However, *Summers et al.* [*2014*] presented the result that hiss spectra produced from high time-resolution "burst" waveform data from the Van Allen Probes occasionally show highly polarized, coherent (over a few wave periods) rising and falling tones. Structured hiss emissions are strongly associated with intervals of high solar wind pressure, and at larger L they can be highly oblique and have large amplitudes [*Tsurutani et al., 2015*].

EMIC waves, also traditionally characterized as structureless, are occasionally observed containing coherent, triggered emissions [*Pickett et al., 2010*; *Grison et al., 2013*; *Nakamura et al., 2014*]. Figure 5 shows examples of these highly structured EMIC waves, observed by *Grison et al.* [*2013*] on Cluster spacecraft, with rising tones reminiscent of whistler mode chorus wave elements. Roughly ~30% of EMIC wave observations from the THEMIS spacecraft beyond 6 RE included rising or falling tones, primarily during larger amplitude events and more disturbed times [*Nakamura et al., 2016*]. Simulations by *Omura and Zhao* [*2013*] have suggested that these EMIC triggered emissions can produce nonlinear trapping and rapid scattering of MeV electrons in the form of relativistic microburst precipitation. During an intense EMIC wave event observed by the Van Allen Probes, *Engebretson et al.* [*2015*] found signatures of relativistic electron depletions in the outer belt qualitatively consistent with the nonlinear trapping theory by *Omura and Zhao* [*2012, 2013*]. *Remya et al.* [*2015*] show that large amplitude (nT), coherent EMIC waves can result in relativistic electron loss rates orders of magnitude higher than those produced by incoherent waves, suggesting that estimates of EMIC scattering should take into account wave coherence and structure.

Figure 5 (from *Grison et al., 2013*): Structured EMIC waves observed simultaneously on three Cluster satellites.
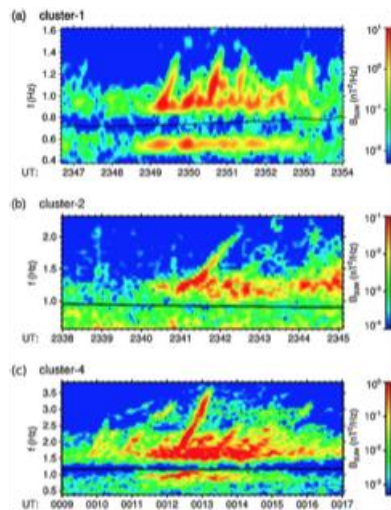
3.1.4 Large amplitude waves

Wave power, though not affecting the conditions of cyclotron resonance, can have a large effect on scattering rates. Under the quasi-linear paradigm, diffusive scattering is proportional to

wave magnetic field power. However, interaction between large amplitude waves and electrons is fundamentally nonlinear, and under these conditions electron transport towards the loss cone may be advective, rather than stochastic.

Unfortunately, the occurrences and properties of large amplitude waves are poorly understood. Time- and frequency-averaged spectral data, traditionally used to study wave properties, overwhelmingly show populations of small amplitude (e.g. $B_w << B_o$), broadband waves, consistent with assumptions inherent in quasi-linear theory. Modern measurements using high cadence resolution "burst" spectra or waveforms, which have much greater time and frequency resolution, often show a much larger range of wave amplitudes on short timescales. Perhaps the most dramatic example of this was the discovery by *Cattell et al.,* [*2008*] of extremely large amplitude (hundreds of mV/m) chorus waves using STEREO satellite burst waveform captures. These waves can carry orders of magnitude more Poynting flux [*Santolik et al., 2010*] than their smaller amplitude counterparts, and can have an unusually large, nonlinearly steepened parallel (to the magnetic field) electric field component [*Agapitov et al., 2018b*] . Due to chorus element inter-spacings, time-averaged amplitudes can under represent true peak amplitudes by an order of magnitude or more [*Cully et al., 2008*; *Tsurutani et al., 2009*].

This discovery has prompted a closer look at past burst waveform datasets for large amplitude chorus [*Wilson et al., 2011*; *Kellogg et al., 2011; Cattell et al., 2012*], as well as for other types of waves. Recent observations show that plasmaspheric hiss waves can be large amplitude, coherent, and oblique on the dayside during times of enhanced magnetospheric compression caused by high solar wind ram pressure [*Tsurutani et al., 2015; Su et al., 2017*]. EMIC waves, which can occur with amplitudes up to a few 10s nT [e.g. *Engebretson et al. 2015*], can also exhibit nonlinear formation and interaction with particles [*Shoji and Omura, 2013*; *Tsintsadzee et al., 2010*], potentially actually reducing their effectiveness as a loss mechanism [*Albert and Bortnik, 2009; Liu et al., 2012*].

Large amplitude waves, though far less common than small amplitude waves, may play an important role in radiation belt electron energization and loss. They can cause phase bunching and phase trapping [*Albert et al., 2002*; *Bortnik et al., 2008; Kellogg et al., 2011*], and dramatic acceleration of electrons [*Mozer et al., 2014*]. Further studies over full solar cycle are needed to quantify wave properties such as amplitudes, periodicities, subpacket structure, and the conditions under which they grow to large amplitudes. This will help to fully understand the role large amplitude waves play in radiation belt dynamics.

3.2 New (multi-payload) observations of wave/precipitation characteristics

Connecting wave-induced loss cone scattering of electrons to observed precipitation is difficult to do with single-satellite instrumentation. Near the magnetic equator where hiss, chorus and EMIC amplitudes typically maximize, the size of the loss cone (~a few degrees at L=5) is often smaller than the angular resolution of particle detectors, thus making it difficult or impossible to distinguish between magnetically trapped and loss cone electrons. Due to this limitation, relating electron loss rates to observed wave populations is then often done by comparing equatorial wave and trapped electron decay rates. Unfortunately, this technique is often unable to distinguish between actual precipitation loss and apparent loss due to energization/de-energization or transport.

Direct comparisons of precipitating electrons to waves requires combining low altitude and high-altitude measurements. Low altitude balloons, ground observatories, and LEO satellites

directly measure precipitating (bounce loss cone) electrons or their atmospheric signatures. These observations can then be compared to comprehensive wave observations, making use of the ever-increasing numbers of satellites and constellation missions in the Earth's magnetosphere - e.g. four Cluster, five THEMIS, two Van Allen Probes, and four MMS satellites - to provide more event-specific loss and scattering comparisons. Multipoint observations allow the resolution of radiation belt evolution on timescales of minutes to hours, less than the orbital period of any single equatorial satellite. In addition, multipoint observations made simultaneously by magnetically conjugate platforms can be used to disentangle spatial from temporal variability of waves and precipitation. These combined measurements allow a more detailed comparison between observations and theory. We now discuss comparative low and high-altitude observations in the context of precipitation associated with plasmaspheric hiss, chorus, and EMIC waves.

3.2.1 Linking precipitation and plasmaspheric hiss observations:

It has been observed for decades that, statistically, the slow (days to weeks) decay of trapped radiation belt electron populations during storm recovery phase is consistent with predicted diffusive scattering loss by plasmaspheric hiss. A more direct comparison of hiss to precipitation loss was provided by *Rodger et al.* [*2007*], who showed that >150 keV precipitating electron fluxes estimated from sub-ionospheric radio signal propagation at L=3.2, and plasmaspheric hiss amplitudes observed on DEMETER had similar order of magnitude day/night asymmetries for a six day storm recovery, suggesting that hiss waves were primarily responsible for this storm recovery.

Jaynes et al. [*2015*] compared precipitating electrons measured on the CCSWE CubeSat [*X. Li et al., 2013*] to trapped populations observed on the Van Allen Probes during a period of low geomagnetic activity where loss contributions from hiss, estimated from Van Allen Probes measurements, could be isolated. Electron lifetimes near L=4.5 were observed to be less than three days, consistent with loss estimates from the observed hiss, but shorter than values typically used in models at the time.

The most direct comparison of plasmaspheric hiss to electron loss was made by *Breneman et al.* [*2015*], who compared BARREL balloon [*Millan et al., 2013*] and Van Allen Probe observations during two intervals of close magnetic conjunction. Distinctive double-peaked modulations (Figure 6) observed in both hiss intensity and electron precipitation up to 180 keV (inferred from the balloon X-ray spectrum) during one of these conjunctions showed a direct connection between hiss and precipitation, with observed loss rates consistent with estimates from quasi-linear theory. These modulations, also observed in plasma density and magnetic field [see also *J. Li et al., 2017*] were near global in scale, as observed from multiple balloons, satellites, and ground magnetometers. These results show that intricate cross--scale wave--wave coupling can significantly modulate both wave intensities and precipitation loss. Similar comparisons of hiss and precipitation at energies >180 keV are necessary for exploring the full energy extent of the influence of plasmaspheric hiss on scattering loss.

Figure 6 (from *Breneman et al., 2017*): Global-scale coherence observed in plasmaspheric hiss and <180 keV precipitation observed during a close magnetic conjunction between Van Allen Probe A and a BARREL balloon. (a) Magnetic field spectral power of hiss showing distinctive

modulations from ~20 Hz to 400 Hz. (b) Comparison of hiss intensity and X-ray counts showing strong similarities for two hours.
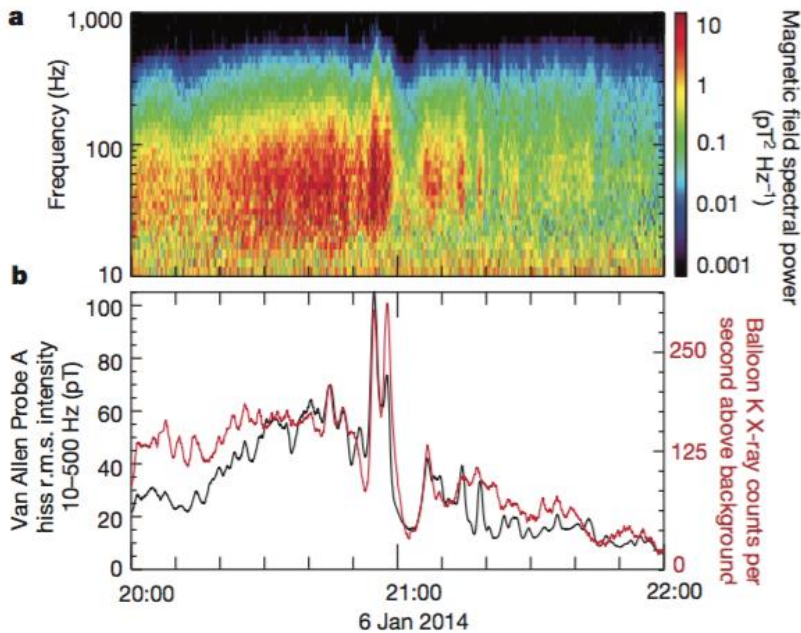
3.2.2 Linking precipitation and chorus observations:

Direct comparisons of chorus to precipitation is, in general, more difficult than for hiss due to its stronger spatial and temporal variability. At sub-relativistic energies, multi-point observations have firmly established the role chorus plays in precipitation loss of 10s keV pulsating aurora [*Nishimura et al., 2010; Kasahara et al., 2018*], microbursts [*Rosenberg et al., 1971*; *Rosenberg et al., 1981*], and regional precipitation [*Lam et al., 2010*; *Halford et al., 2015b*]. Measurements of >30 keV precipitating electron flux on the POES LEO constellation are now routinely used to infer equatorial amplitudes [*Li et al., 2013b*; *Ni et al., 2014b*].

Observations are sparser at relativistic energies, largely due to lower flux levels and lack of energy coverage/resolution on low altitude particle detectors. Chorus is perhaps the leading wave candidate for the creation of relativistic microbursts from ~100 keV to up to ~MeV. Large-scale regions producing chorus and precipitation can last for hours and extend across multiple L and MLT. [*Anderson et al., 2017*]. These regions are constrained beyond the plasmapause, typically across the morningside, and have occurrences that increase with geomagnetic activity [*Johnston and Anderson 2010*]. Within these extended generation regions, smaller chorus and microburst substructures are observed [*Kersten et al., 2011*; *Aryan et al., 2016*; *Anderson et al., 2017*], though their relation has not been established.

On smaller scales, individual chorus subpackets and microbursts share similar durations and cadences. Spatial scales perpendicular to the background magnetic field, as determined from simultaneous multipoint measurements, range from many tens [*Santolik et al., 2003, Santolik et al., 2004a*] to more than a thousand km [*Agapitov et al. 2011*; *Agapitov et al., 2017*]. When mapped to the topside ionosphere, these scales are roughly consistent with the few to 10s km scale size of individual relativistic microbursts, inferred from single spacecraft [e.g. *Blake et al., 2096*] and multipoint CubeSats [*Crew et al., 2016*] measurements.

Direct comparison of chorus to microbursts is difficult, however, due to this small transverse scale size. *Breneman et al.* [*2017*] provided the first direct evidence that lower band, rising tone chorus waves create relativistic microbursts by analyzing a near-perfect magnetic conjunction between Van Allen Probe A and one of two FIREBIRD II CubeSats [*Klumpar et al., 2015*]. The combined datasets showed that the chorus created microbursts over a wide energy range from 200-850 keV along a single magnetic field line. The likely mechanism was n=-1 cyclotron resonance scattering away from the chorus source at 20-30° mlat, consistent with the theoretical suggestion of *Thorne et al.* [*2005*], and with quasi-linear [*Shprits et al., 2009*] and nonlinear test particle simulations [*Hikishima et al., 2010*; *Saito et al., 2012*]. Comparisons of the microburst flux to the trapped electron population at L=5.6 showed that a long-lasting chorus source region extended over a few hours MLT, consistent observations of *Anderson et al., 2017*, would provide a major source of radiation belt electron loss from 200-850 keV. Using SAMPEX measurements of >1 MeV electrons, *Douma et al.* [*2018*] found microburst events in close conjunction with VLF signatures suggestive of chorus observed on the ground, but also found some with ground observations of EMIC waves, suggesting that, on occasion, some MeV microbursts may be caused by EMIC rather than chorus waves.

At lower energies, *Mozer et al.* [*2018*] compared Van Allen Probe B and AC6-B CubeSat [*Blake and O'Brien, 2016*] observations mapping to the same patchy region of larger precipitation showing strongly correlated one second averages of chorus and >35 keV microbursts. These scattering interactions must be fundamentally nonlinear due to the large (1 nT) chorus amplitudes, but observed fluxes were shown to be consistent with quasi-linear scattering rates, suggesting that the overall effect of many nonlinear scattering interactions can resemble quasi-linear diffusion [also see *Tao et al., 2012*].

The aforementioned multipoint studies provide strong evidence that chorus creates microbursts from sub-relativistic (10s keV) to relativistic (~MeV) energies. However, due to the small number of comparative studies, many details of this connection remain unresolved. Examples include small-scale spatial structures, termed *curtains* [*Blake and O'Brien, 2016*], thought to come about from drift loss cone microburst populations, microburst energy and storm phase dependence, and the overall importance of relativistic microbursts to outer belt electron loss.

3.2.3 Linking precipitation and EMIC observations:

Direct links between EMIC waves and relativistic electron precipitation have increasingly been observed with recent multi-observatory measurements. Early observations of REP events preferentially occurring on the duskside, close to the plasmapause, provided the first suggestion of their connection to EMIC waves [e.g. *Imhof et al., 1986*; *Millan et al., 2002*]. The narrow radial extent of REP events observed by LEO spacecraft is consistent with the often radially narrow EMIC wave spatial extents suggested by combined ground and in situ wave observations [e.g. *Mann et al., 2014; Paulson et al., 2014*]. Multipoint in situ observations have now begun to quantify these spatial and temporal extents of EMIC waves [e.g. *Lee et al., 2013*; *Clausen et al., 2011*; *Engebretson et al., 2008; Engebretson et al., 2015*; *Sigsbee et al., 2016*; *Blum et al., 2017*; *Yu et al., 2017*], for better comparison to precipitation region properties. Multipoint observations of REP regions, e.g. from the BARREL balloon and POES satellite constellations, suggest that precipitation events are often very localized [*Shekhar et al., 2017*; *Millan et al., 2016* AGU abstract]

Recent coordinated observations of EMIC wave activity have been seen at locations magnetically conjugate to simultaneously observed REP events, further strengthening their association. EMIC waves were observed by ground-based magnetometers in conjunction with keV ion and MeV electron precipitation [*Miyoshi et al., 2008; Hendry et al., 2016*] as well as with ground-based electron precipitation signatures [*Rodger et al. 2008*]. However, due to ducting of EMIC waves as they propagate to lower altitudes, it can be difficult to identify the localized region in space of wave generation from ground observations [*Greifinger and Greifinger, 1968*; *Fujita and Tamao, 1988*]. More recently, studies have observed precipitation in close magnetic conjunction with in situ EMIC waves near the equator, often with similar modulation between precipitation and waves [*Z. Li et al., 2014*; *Blum et al., 2015b*; *Rodger et al., 2015*]. Applying quasilinear theory to observed EMIC wave properties measured near the equator, *Z. Li et al.* [*2014*] were able to reproduce the precipitation signature observed at one of the BARREL balloons during an event in Jan 2013. These event studies have confirmed that at least some REP events are produced by EMIC wave scattering in the magnetosphere. Quantification of precipitation due to these events [e.g. *Blum et al., 2013*] suggests they can provide significant loss to the localized L shells over which they occur, in agreement with the minima in PSD profiles observed by *Shprits et al.* [*2017*].

Through these conjugate studies, additional questions have arisen regarding the nature of the relationship between EMIC waves and REP. While individual events confirm that EMIC waves can produce REP events seen by balloons, LEO spacecraft, and ground-based platforms, the global distributions of EMIC waves and REP events show significant differences - with EMIC wave occurrences peaking in the noon and afternoon sectors, while REP events show a pre-midnight occurrence peak [e.g. *Smith et al., 2016*]. It is necessary to determine what fraction of EMIC waves produce relativistic electron precipitation, and what fraction of these precipitation events are due to EMIC wave scattering. While field line curvature scattering was initially proposed as a process producing MeV electron precipitation on the nightside [*Imhof et al., 1991*], *Smith et al.* [*2016*] suggested this might also produce some of the coincident MeV electron and keV proton precipitation features often interpreted as due to EMIC wave scattering.

The energy spectrum and structure of EMIC wave-driven precipitation is also an open topic of investigation. A number of REP events show precipitating energy spectra peaked at ~1-2 MeV [*Z. Li et al., 2014*; *Woodger et al., 2015*; *Clilverd et al., 2017*], in agreement with theoretical estimates than EMIC waves primarily scatter electrons above a ~MeV minimum resonant energy [*Thorne and Kennel, 1971*]. However, a handful of studies have found evidence of sub-MeV electron precipitation, down to energies at low as ~300 keV, in association with EMIC waves [*Clilverd et al., 2015*; *Hendry et al., 2017*]. EMIC wave anomalous cyclotron resonant scattering of these low energies can only occur under extreme, likely unrealistic, plasma and field conditions; however, non-resonant or bounce resonance interactions might allow EMIC waves to scatter electrons at these lower energies [*Chen et al., 2016*; *Cao et al., 2017*]. This motivates investigation into the detailed nature of the wave-particle interaction and precipitating electron energy spectrum driven by EMIC waves

Together, recent conjugate wave and precipitation studies have helped solidify the causal relationship between various types of waves and precipitation events. However, new questions have arisen from these observations, and continued study of such events will enable more detailed understanding of the energy spectrum, spatial structure, and global distributions of different types of precipitation and their drivers.

4: Discussion and Conclusions

4.1 **Incorporating cyclotron resonant scattering into radiation belt models**

Comprehensive datasets provided by the single- and multi-point observations discussed in Section 3 are necessary for constraining radiation belt models, which facilitate our understanding of radiation belt dynamics. Models are only as good as the accuracy of the empirical data that drives them, and incomplete knowledge of diffusion coefficients, for example, can lead to significant, even orders of magnitude uncertainties in electron lifetimes [e.g. *Tu et al., 2013*; *Pham et al., 2017*; *Agapitov et al., 2018a*]. Input with the aforementioned up-to-date wave distributions, parameterized with respect to spatial location and activity level [e.g. *Shprits et al., 2007*; *Spasojevic et al., 2013*], modern simulations show relatively good agreement with comprehensive observations of radiation belt electron decay on multi-day timescales. They also provide further support of the general importance of resonant scattering by hiss, chorus, and EMIC waves.

Further improvements to parameterization are being explored. Hiss and chorus wave populations, for example, are bounded inside and outside the plasmasphere, respectively, and sorting their properties relative to plasma boundaries, rather than strict L, which varies only statistically with L, is a more natural system, as shown in Figure 7 [*Malaspina et al., 2016*]. Parameterizations of waves relative to the plasmapause location have not yet been integrated into quasi-linear diffusion models, but may significantly enhance their accuracy during highly dynamic times.

Figure 7 (from *Malaspina et al., 2016*): Comparative sorting of plasmaspheric hiss and chorus wave power by L-shell and distance relative to the plasmapause (delta-L). (a and b) Wave power sorted traditionally by L-shell, and (c and d) wave power sorted relative to distance from the plasmapause, which provides a clear delineation of wave power.
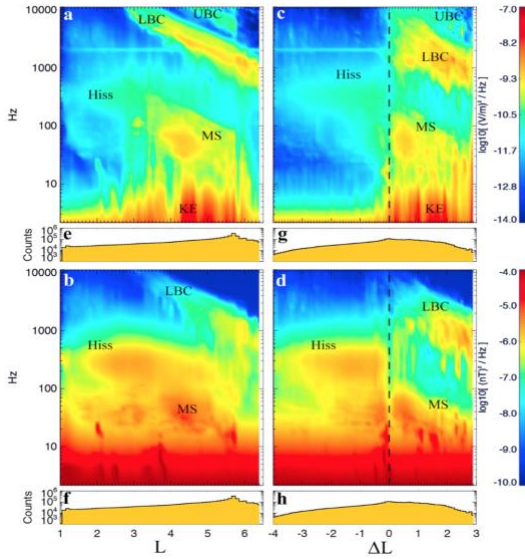
Despite all these improvements, using statistical models to describe radiation belt evolution has severe limitations. Some waves, due to their sporadic nature - like EMIC waves [*Drozdov et al., 2017*] or <100 Hz hiss [*Malaspina et al., 2017*] - are difficult to properly parameterize. In addition, stormtime radiation belts often show significant variation on timescales of minutes and hours [e.g. *Yu et al., 2015*], which cannot be accurately captured using empirical models based on highly averaged data. Instead, event-specific waves, particles, and plasma boundaries with good spatial, energy, and time resolution are needed [*Thorne et al., 2013*; *Tu et al., 2014*; *Xiao et al., 2015*; *Schiller et al., 2017*]. This allows models to differentiate between different important physical processes. For example, certain dramatic outer belt electron flux dropouts (not caused by outer boundary loss) during storms [e.g. *Morley et al., 2010*] require either consideration of nonlinear scattering loss, or more accurate input to QL models with high spatiotemporal, and energy resolution input. This necessitates a better quantification of REP [e.g. *Shekhar et al., 2017*].

4.2 Summary

In this review, we discuss the role of wave-particle interactions in driving loss of radiation belt electrons, with an emphasis on observational signatures of this process. These include direct measurements of precipitation, wave properties, and variations in the trapped electron population as a result of cyclotron resonance.

Precipitation loss from cyclotron resonance with plasma waves, primarily hiss, chorus, and EMIC, is one of the primary drivers of radiation belt morphology. The energy-dependent structure of the slot region and inner belt is formed primarily by the balance of inward radial transport and scattering loss from plasmaspheric hiss. In the outer belt, and outside of the plasmasphere, chorus waves can cause significant scattering loss over a wide range of energies. EMIC waves, not limited by the plasmapause boundary, likely control loss of ultra-relativistic electrons. While the role of these three waves in forming the large-scale structure of the belts is well-established, their contributions to the more complex dynamics and fine-scale features recently observed are still under investigation.

Sophisticated wave instrumentation on recent satellite missions has provided new details of wave properties, including observations of large amplitude, highly oblique waves, power at extended frequency ranges, and previously undiscovered wave coherence and structure. These observations motivate revisiting theories of wave particle interactions and the contribution of these waves to radiation belt electron loss and overall dynamics.

Lastly, a new paradigm of simultaneous multi-platform observations, including equatorial and LEO satellites, balloons, and ground-based observations, has led to new insights into wave-induced precipitation. These observations show temporal and large-scale spatial structures of waves and precipitation. Simultaneous, magnetically conjugate measurements allow close comparisons of scattering by various wave types and electron precipitation loss, vital for understanding the relative roles played by various wave types. Investigation continues into the energy dependence of precipitation events, as well as when, where, and how often various wave modes cause different types of precipitation.

Ultimately, the importance of precipitation loss, including inter-comparison of different precipitation loss processes, cannot be ascertained without careful consideration of other time-dependent loss processes, such as outward radial diffusion and magnetopause shadowing [e.g. *Tu et al., 2013*; *Murphy et al., 2016*; *Watt et al., 2017*; *Mann et al., 2016b*], and second that care must be taken when generalizing modern results due to the historically quiet solar cycle 23 [*Russell et al., 2010*] and relatively quiet cycle 24 [*X. Li et al., 2017*; *Riley and Love, 2017*].

BIBLIOGRAPHY

Abel, B., and R. M. Thorne (1998), Electron scattering loss in Earth's inner magnetosphere: 1. Dominant physical processes, J. Geophys. Res., 103(A2), 2385–2396, doi:10.1029/97JA02919.

Agapitov, O., V. Krasnoselskikh, T. Dudok de Wit, Y. Khotyaintsev, J. S. Pickett, O. Santolík, and G. Rolland (2011), Multispacecraft observations of chorus emissions as a tool for the plasma density fluctuations' remote sensing, J. Geophys. Res., 116, A09222, doi:10.1029/2011JA016540.

Agapitov, O., A. Artemyev, V. Krasnoselskikh, Y. V. Khotyaintsev, D. Mourenas, H. Breuillard, M. Balikhin, and G. Rolland (2013), Statistics of whistler-mode waves in the outer radiation belt: Cluster STAFF-SA measurements, J. Geophys. Res. Space Physics, 118, 3407–3420, doi:10.1002/jgra.50312.

Agapitov, O. V., A. V. Artemyev, D. Mourenas, Y. Kasahara, and V. Krasnoselskikh (2014), Inner belt and slot region electron lifetimes and energization rates based on AKEBONO statistics of whistler waves, *J. Geophys. Res. Space Physics*, *119*, 2876–2893, doi:10.1002/2014JA019886.

Agapitov, O. V., A. V. Artemyev, D. Mourenas, F. S. Mozer, and V. Krasnoselskikh (2015), Nonlinear local parallel acceleration of electrons through Landau trapping by oblique whistler mode waves in the outer radiation belt, *Geo- phys. Res. Lett.*, *42*, 10,140–10,149, doi:10.1002/2015GL066887.

Agapitov, O., L. W. Blum, F. S. Mozer, J. W. Bonnell, and J. Wygant (2017), Chorus whistler wave source scales as determined from multipoint Van Allen Probe measurements, Geophys. Res. Lett., 44, 2634–2642, doi:10.1002/ 2017GL072701.

Agapitov, O. V., Mourenas, D., Artemyev, A. V., Mozer, F. S., Hospodarsky, G., Bonnell, J., & Krasnoselskikh, V. (2018a). Synthetic empirical chorus wave model from combined Van Allen Probes and Cluster statistics, Journal of Geophysical Research: Space Physics, 123. https://doi.org/10.1002/2017JA024843

Agapitov, O., Drake, J. F., Vasko, I., Mozer, F. S., Artemyev, A., Krasnoselskikh, V., et al. (2018b). Nonlinear electrostatic steepening of whistler waves: The guiding factors and dynamics in inhomogeneous systems. Geophysical Research Letters, 45, 2168–2176. https://doi.org/10.1002/2017GL076957

Albert, J. M., Quasi-linear pitch angle diffusion coefficients: Retaining high harmonics (1994), J. Geophys. Res., 99(A12), 23741–23745, doi:10.1029/94JA02345.

Albert, J. M. (2002), Nonlinear interaction of outer zone electrons with VLF waves, Geophys. Res. Lett., 29(8), 1275, doi:10.1029/ 2001GL013941.

Albert, J. M. (2003), Evaluation of quasi-linear diffusion coefficients for EMIC waves in a multispecies plasma, J. Geophys. Res., 108(A6), 1249, doi:10.1029/2002JA009792.

Albert, J.M., and Shprits, Y.Y (2008), Estimates of lifetimes against pitch angle diffusion, 71(16), Pages 1647-1652, https://doi.org/10.1016/j.jastp.2008.07.004

Albert, J.M., and Shprits, Y.Y. (2009), Estimates of lifetimes against pitch angle diffusion, Journal of Atmospheric and Solar-Terrestrial Physics 71 (2009) 1647–1652

Albert, J. M. (2010), Diffusion by one wave and by many waves, J. Geophys. Res., 115, A00F05, doi:10.1029/2009JA014732.

Albert, J. M. (2012), Dependence of quasi-linear diffusion coefficients on wave parameters, J. Geophys. Res., 117, A09224, doi:10.1029/2012JA017718.

Albert, J. M., M. J. Starks, R. B. Horne, N. P. Meredith, and S. A. Glauert (2016), Quasi-linear simulations of inner radiation belt electron pitch angle and energy distributions, *Geo-phys. Res. Lett.*, *43*, 2381–2388, doi:10.1002/2016GL067938.

Albert, J. M. (2017), Quasi-linear diffusion coefficients for highly oblique whistler mode waves, *J. Geophys. Res. Space Physics*, *122*, doi:10.1002/2017JA024124.

Albert, J. M., and J. Bortnik (2009), Nonlinear interaction of radiation belt electrons with electromagnetic ion cyclotron waves, Geophys. Res. Lett., 36, L12110, doi:10.1029/2009GL038904.

Allen, R. C., J.-C. Zhang, L. M. Kistler, H. E. Spence, R.-L. Lin, B. Klecker, M. W. Dunlop, M. André, and V. K. Jordanova (2015), A statistical study of EMIC waves observed by Cluster: 1. Wave properties, J. Geophys. Res. Space Physics., 120, doi:10.1002/2015JA021333.

Anderson, B. R., S. Shekhar, R. M. Millan, A. B. Crew, H. E. Spence, D. M. Klumpar, J. B. Blake, T. P. O'Brien, and D. L. Turner (2017), Spatial scale and duration of one microburst region on 13 August 2015, *J. Geophys. Res. Space Physics*, *122*, doi:10.1002/2016JA023752.

Artemyev, A., O. Agapitov, H. Breuillard, V. Krasnoselskikh, and G. Rolland (2012a), Electron pitch-angle diffusion in radiation belts: The effects of whistler wave oblique propagation, Geophys. Res. Lett., 39, L08105, doi:10.1029/ 2012GL051393.

Artemyev, A.V., Krasnoselskikh, V.V., Agapitov, O.V., Mourenas, D., Rolland, G. (2012b), Non diffusive resonant acceleration of electrons in the radiation belts, Physics of Plasmas, 19, 122901

Artemyev, A.V., Agapitov, O.V., Mourenas, D., Krasnoselskikh, V.V., Mozer, F.S. (2015), Wave energy budget analysis in the Earth's radiation belts uncovers a missing energy, Nature Comm., 6, 8143, doi:10.1038/ncomms8143

Artemyev, A., Agapitov, O., Mourenas, D., Krasnoselskikh, V., Shastun, V., Mozer, F. (2016), Oblique Whistler-Mode Waves in the Earth's Inner Magnetosphere: Energy Distribution, Origins, and Role in Radiation Belt Dynamics , Space Sci Rev (2016) 200:261–355 DOI 10.1007/s11214-016-0252-5

Aryan, H., D. Sibeck, M. Balikhin, O. Agapitov, and C. Kletzing (2016), Observation of chorus waves by the Van Allen Probes: Dependence on solar wind parameters and scale size, *J. Geophys. Res. Space Physics*, *121*, 7608–7621, doi:10.1002/2016JA022775.

Baker, D.N. et al., (2012), Solar and Space Physics: A Science for a Technological Society, Committee on a Decadal Strategy for Solar and Space Physics (Heliophysics); Space Studies Board; Aeronautics and Space Engineering Board; Division of Earth and Physical Sciences; National Research Council

Baker, D.N., et al. (2013), A Long-Lived Relativistic Electron Storage Ring Embedded in Earth's Outer Van Allen Belt, Science, Vol. 340, Issue 6129, pp. 186-190, DOI: 10.1126/science.1233518.

Baker, D. N., et al. (2014a), Gradual diffusion and punctuated phase space density enhancements of highly relativistic electrons: Van Allen Probes observations, Geophys. Res. Lett., 41, 1351–1358, doi:10.1002/2013GL058942.

Baker, D.N., et al. (2014b), An impenetrable barrier to ultra-relativistic electrons in the Van Allen radiation belts, Nature, doi:10.1038/nature13956

Bellan, P.M., Pitch angle scattering of an energetic magnetized particle by a circularly polarized electromagnetic wave (2013), Physics of Plasmas **20**, 042117, https://doi.org/10.1063.1.4801055

Blake, J.B., Looper, M.D., Baker, D.N., Nakamura, R., Klecker, B., Hovestadt, D. (1996), New high temporal and spatial resolution measurements by SAMPEX of the precipitation of relativistic electrons, https://doi.org/10.1016/0273-1177(95)00969-8

Blake, J.B., Looper, M.D., Baker, D.N., Nakamura, R., Klecker, B., Hovestadt, D. (2012)**,** New high temporal and spatial resolution measurements by SAMPEX of the precipitation of relativistic electrons, https://doi.org/10.1016/0273-1177(95)00969-8**.**

Blake, J. B., and T. P. O'Brien (2016), Observations of small-scale latitudinal structure in energetic electron precipi- tation, J. Geophys. Res. Space Physics, 121, 3031–3035, doi:10.1002/ 2015JA021815.

Blum, L. W., Q. Schiller, X. Li, R. Millan, A. Halford, and L. Woodger (2013), New conjunctive CubeSat and balloon measurements to quantify rapid energetic electron precipitation, Geophys. Res. Lett., 40, 5833–5837, doi:10.1002/2013GL058546.

Blum, L., X. Li, and M. Denton (2015a), Rapid MeV electron precipitation as observed by SAMPEX/HILT during high-speed stream-driven storms, $_{SEP}$J. Geophys. Res. Space Physics, 120, doi:10.1002/2014JA020633.

Blum, L. W., et al. (2015b), Observations of coincident EMIC wave activity and duskside energetic electron precipitation on 18–19 January 2013, Geophys. Res. Lett., 42, 5727–5735, doi:10.1002/2015GL065245.

Blum, L. W., J. W. Bonnell, O. Agapitov, K. Paulson, and C. Kletzing (2017), EMIC wave scale size in the inner magnetosphere: Observations from the dual Van Allen Probes, Geophys. Res. Lett., 44, doi:10.1002/2016GL072316.

Bortnik, J., U. S. Inan, and T. F. Bell (2003), Frequency-time spectra of magnetospherically reflecting whistlers in the plasmasphere, J. Geophys. Res., 108(A1), 1030, doi:10.1029/2002JA009387.

Bortnik, J., Thorne, R.M., The dual role of ELF/VLF chorus waves in the acceleration and precipitation of radiation belt electrons (2007), Journal of Atmospheric and Solar-Terrestrial Physics 69, 378–386.

Bortnik, J., R. M. Thorne, and U. S. Inan (2008), Nonlinear interaction of energetic electrons with large amplitude chorus, Geophys. Res. Lett., 35, L21102, doi:10.1029/ 2008GL035500.

Bortnik, J., L. Chen, W. Li, R. M. Thorne, and R. B. Horne (2011), Modeling the evolution of chorus waves into plasmaspheric hiss, J. Geophys. Res., 116, A08221, doi:10.1029/2011JA016499.

Boynton, R. J., Mourenas, D., & Balikhin, M. A. (2017). Electron flux dropouts at $L \sim 4.2$ from Global Positioning System satellites: Occurrences, magnitudes, and main driving factors. *Journal of Geophysical Research: Space Physics*, *122*. https://doi.org/10.1002/2017JA024523.

Brautigam, D. H., and J. M. Albert (2000), Radial diffusion analysis of outer radiation belt electrons during the October 9, 1990, magnetic storm, J. Geophys. Res., 105(A1), 291–309, doi:10.1029/1999JA900344.

Breneman, A.W., Halford, A., Millan, R., McCarthy, M., Fennell, J., Sample, J., Woodger, L., Hospodarsky, G., Wygant, J.R., Cattell, C.A., Goldstein, J., Malaspina, D., Kletzing, C.A. (2015), Global-scale coherence modulation of radiation-belt electron loss from plasmaspheric hiss, Nature, 523, 193-195, doi:10.1038/nature14515.

Breneman A. et al., (2017), Observations directly linking relativistic electron microbursts to whistler mode chorus: Van Allen Probes and FIREBIRD II, Geophys. Res. Lett., 44, doi:10.1002/2017GL075001.

Brice, N. (1964), Fundamentals of very low frequency emission generation mechanisms, J. Geophys. Res., 69(21), 4515–4522, doi:10.1029/JZ069i021p04515.

Brown, J.W., and Stone, E.C. (1972), High-energy electron spikes at high latitudes 77, 3384–3396, 10.1029/JA077i019p03384

Burtis, W.J., and Helliwell, R.A. (1969), Banded chorus- A new type of VLF radiation observed in the magnetosphere by OGO 1 and OGO 3, J. Geophys. Res., 74(11)

Burton, R. K., and R. E. Holzer (1974), The origin and propagation of chorus in the outer magnetosphere, J. Geophys. Res., 79(7), 1014–1023, doi:10.1029/JA079i007p01014.

Cao, X., et al. (2017), Bounce resonance scattering of radiation belt electrons by H+ band EMIC waves, J. Geophys. Res. Space Physics, 122, doi:10.1002/ 2016JA023607.

Carson, B. R., C. J. Rodger, and M. A. Clilverd (2013), POES satellite observations of EMIC-wave driven relativistic electron precipitation during 1998–2010, *J. Geophys. Res. Space Physics*, *118*, 232–243, doi:10.1029/2012JA017998.

Cattell, C., et al. (2008), Discovery of very large amplitude whistler-mode waves in Earth's radiation belts, Geophys. Res. Lett., 35, L01105, doi:10.1029/2007GL032009

Cattell, C. A., Breneman, A., Goetz, K., Kellogg, P. J., Kersten, K., Wygant, J. R., Wilson, L. B., Looper, M. D., Blake, J.B. and Roth, I. (2012) Large-Amplitude Whistler Waves and Electron Acceleration in the Earth's Radiation Belts: A Review of Stereo and Wind Observations, in Dynamics of the Earth's Radiation Belts and Inner Magnetosphere (eds D. Summers, I. R. Mann, D. N. Baker and M. Schulz), American Geophysical Union, Washington, D. C. doi: 10.1029/2012GM001322

Cattell, C. A., A. W. Breneman, S. A. Thaller, J. R. Wygant, C. A. Kletzing, and W. S. Kurth (2015), Van Allen Probes observations of unusually low frequency whistler mode waves observed in association with moderate magnetic storms: Statistical study, Geophys. Res. Lett., 42, 7273–7281, doi:10.1002/2015GL065565.

Chaston, C. C., et al. (2014), Observations of kinetic scale field line resonances, Geophys. Res. Lett., 41, 209–215, doi:10.1002/2013GL058507.

Chen, L., O. Santolík, M. Hajoš, L. Zheng, Z. Zhima, R. Heelis, M. Hanzelka, R. B. Horne, and M. Parrot (2017), Source of the low-altitude hiss in the ionosphere, *Geophys. Res. Lett.*, *44*, 2060–2069, doi:10.1002/2016GL072181.

Chen, L., R. M. Thorne, and R. B. Horne (2009), Simulation of EMIC wave excitation in a model magnetosphere including structured high-density plumes, *J. Geophys. Res.*, *114*, A07221, doi:10.1029/2009JA014204.

Chen, L., J. Bortnik, W. Li, R. M. Thorne, and R. B. Horne (2012), Modeling the properties of plasmaspheric hiss: 1. Dependence on chorus wave emission, J. Geophys. Res., 117, A05201, doi:10.1029/2011JA017201.

Chen, L., et al. (2014), Generation of unusually low frequency plasmaspheric hiss, *Geophys. Res. Lett.*, *41*, 5702–5709, doi:10.1002/2014GL060628.

Chen, L., R. M. Thorne, J. Bortnik, and X.-J. Zhang (2016), Nonresonant interactions of electromagnetic ion cyclotron waves with relativistic electrons, *J. Geophys. Res. Space Physics*, *121*, 9913–9925, doi:10.1002/2016JA022813.

Chen, Y., Reeves, G. D., Friedel, R.H.W. (2007), The energization of relativistic electrons in the outer Van Allen radiation belt, *Nature Physics* 3, 614–617, doi:10.1038/nphys655.

Chen, L., R. M. Thorne, and J. Bortnik (2011), The controlling effect of ion temperature on EMIC wave excitation and scattering, Geophys. Res. Lett., 38, L16109, doi:10.1029/2011GL048653.

Clausen, L. B. N., J. B. H. Baker, J. M. Ruohoniemi, and H. J. Singer (2011), EMIC waves observed at geosynchronous orbit during solar minimum: Statistics and excitation, J. Geophys. Res., 116, A10205, doi:10.1029/ 2011JA016823.

Clilverd, M. A., N. R. Thomson, and A. J. Smith (1993), The influence of ionospheric absorption on midlatitude whistler-mode signal occurrence from VLF transmitters, J. Atmos. Terr. Phys., 55, 1469 – 1477, doi:10.1016/0021-9169(93)90112-C.

Clilverd, M. A., C. J. Rodger, R. Gamble, N. P. Meredith, M. Parrot, J.-J. Berthelier, and N. R. Thomson (2008), Ground- based transmitter signals observed from space: Ducted or nonducted?, J. Geophys. Res., 113, A04211, doi:10.1029/2007JA012602.

Clilverd, M. A., et al. (2009), Remote sensing space weather events: The AARDDVARK network, Space Weather, 7, S04001, doi:10.1029/ 2008SW000412.

Clilverd, M. A., R. Duthie, R. Hardman, A. T. Hendry, C. J. Rodger, T. Raita, M. Engebretson, M. R. Lessard, D. Danskin, and D. K. Milling (2015), Electron precipitation from EMIC waves: A case study from 31 May 2013, J. Geophys. Res. Space Physics, 120, doi:10.1002/ 2015JA021090.

Clilverd, M. A., C. J. Rodger, M. McCarthy, R. Millan, L. W. Blum, N. Cobbett, J. B. Brundell, D. Danskin, and A. J. Halford (2017), Investigating energetic electron precipitation through combining ground-based and balloon observa- tions, J. Geophys. Res. Space Physics, 122, doi:10.1002/2016JA022812.

Comess, M. D., D. M. Smith, R. S. Selesnick, R. M. Millan, and J. G. Sample (2013), Duskside relativistic electron precipitation as measured by SAMPEX: A statistical survey, J. Geophys. Res. Space Physics, 118, 5050–5058, doi:10.1002/jgra.50481.

Cornwall, J. M. (1965), Cyclotron instabilities and electromagnetic emission in the ultra low frequency and very low frequency ranges, J. Geophys. Res., 70(1), 61–69, doi:10.1029/JZ070i001p00061.

Cornwall, J. M., F. V. Coroniti, and R. M. Thorne (1970), Turbulent loss of ring current protons, J. Geophys. Res., 75, 4699.

Crabtree, C., E. Tejero, G. Ganguli, G. B. Hospodarsky, and C. A. Kletzing (2017), Bayesian spectral analysis of chorus subelements from the Van Allen Probes, *J. Geophys. Res. Space Physics*, *122*, doi:10.1002/2016JA023547.

Crew, A. B., et al. (2016), First multipoint in situ observations of electron microbursts: Initial results from the NSF FIREBIRD II mission, J. Geophys. Res. Space Physics, 121, doi:10.1002/2016JA022485.

Cully, C. M., J. W. Bonnell, and R. E. Ergun (2008), THEMIS observations of long-lived regions of large-amplitude whistler waves in the inner magnetosphere, Geophys. Res. Lett., 35, L17S16, doi:10.1029/2008GL033643.

Darrouzet, F., V. Pierrard, S. Benck, G. Lointier, J. Cabrera, K. Borremans, N. Yu Ganushkina, and J. De Keyser (2013), Links between the plasmapause and the radiation belt boundaries as observed by the instruments CIS, RAPID and WHISPER onboard Cluster, J. Geophys. Res. Space Physics, 118, 4176–4188, doi:10.1002/jgra.50239.

Denton, R. E., M. J. Engebretson, A. Keiling, A. P. Walsh, S. P. Gary, P. M. E. Décréau, C. A. Cattell, and H. Rème (2010), Multiple harmonic ULF waves in the plasma sheet boundary layer: Instability analysis, *J. Geophys. Res.*, **115**, A12224, doi:10.1029/2010JA015928.

Douma, E., C. J. Rodger, L. W. Blum, and M. A. Clilverd (2017), Occurrence characteristics of relativistic electron microbursts from SAMPEX observations, *J. Geophys. Res. Space Physics 122*, 8096–8107, doi:10.1002/ 2017JA024067.

Drozdov, A. Y., Y. Y. Shprits, M. E. Usanova, N. A. Aseev, A. C. Kellerman, and H. Zhu (2017), EMIC wave parameterization in the long-term VERB code simulation, J. Geophys. Res. Space Physics, 122, 8488–8501, doi:10.1002/2017JA024389.

Engebretson, M. J., J. L. Posch, A. M. Westerman, N. J. Otto, J. A. Slavin, G. Le, R. J. Strangeway, and M. R. Lessard (2008), Temporal and spatial characteristics of Pc1 waves observed by ST5, J. Geophys. Res., 113, A07206, doi:10.1029/2008JA013145.

Engebretson, M. J., et al. (2015), Van Allen probes, NOAA, GOES, and ground observations of an intense EMIC wave event extending over 12 h in magnetic local time, J. Geophys. Res. Space Physics, 120, 5465–5488, doi:10.1002/ 2015JA021227.

Engebretson, M., & Zesta, E. (2017). The future of ground magnetometer arrays in support of space weather monitoring and research. Space Weather, 15. https:// doi.org/10.1002/2017SW001718 [SEP]

Foat, J.E. et al. (1998), First detection of a terrestrial MeV X-ray burst, Geophys. Res. Lett., DOI: 10.1029/1998GL900134

Foster, J. C., P. J. Erickson, D. N. Baker, A. N. Jaynes, E. V. Mishin, J. F. Fennel,[SEP] X. Li, M. G. Henderson, and S. G. Kanekal (2016a), Observations of the impenetrable barrier, the plasmapause, and the VLF bubble during the 17 March 2015 storm, J. Geophys. Res. Space Physics, 121, 5537–5548, doi:10.1002/2016JA022509. [SEP]

Foster, J. C., P. J. Erickson, Y. Omura, D. N. Baker, C. A. Kletzing, and S. G. Claudepierre (2016b), Van Allen Probes observations of prompt MeV radiation belt electron acceleration in nonlinear interactions with VLF chorus, *J. Geophys. Res. Space Physics*, *122*, doi:10.1002/2016JA023429.

Fraser, B. J., and T. S. Nguyen (2001), Is the plasmapause a preferred source region of electromagnetic cyclotron waves in the magnetosphere, *J. Atmos. Sol. Terr. Phys.*, *63*, 1225–1247.

Friedel, R.H.W, Reeves, G.D., Obara, T. (2002), Relativistic electron dynamics in the inner magnetosphere — a review, https://doi.org/10.1016/S1364-6826(01)00088-8

Fu, X., et al. (2014), Whistler anisotropy instabilities as the source of banded chorus: Van Allen Probes observations and particle-in-cell simulations, *J. Geophys. Res. Space Physics*, *119*, 8288–8298, doi:10.1002/2014JA020364.

Fujita, S., and T. Tamao (1988), Duct propagation of hydromagnetic waves in the upper ionosphere: 1. Electromagnetic field distributions in high latitudes associated with localized incidence of a shear Alfvén wave, J. Geophys. Res., 93, 14,665–14,673, doi:10.1029/ JA093iA12p14665.

Gamble, R. J., C. J. Rodger, M. A. Clilverd, J.-A. Sauvaud, N. R. Thomson, S. L. Stewart, R. J. McCormick, M. Parrot, and J.-J. Berthelier (2008), Radiation belt electron precipitation by man-made VLF transmissions, J. Geophys. Res., 113, A10211, doi:10.1029/2008JA013369.

Gao, X., W. Li, R. M. Thorne, J. Bortnik, V. Angelopoulos, Q. Lu, X. Tao, and S. Wang (2014), Statistical results describing the bandwidth and coherence coefficient of whistler mode waves using THEMIS waveform data, J. Geophys. Res. Space Physics, 119, 8992–9003, doi:10.1002/2014JA020158.

Gao, Y., F. Xiao, Q. Yan, C. Yang, S. Liu, Y. He, and Q. Zhou (2015), Influence of wave normal angles on hiss-electron interaction in Earth's slot region, *J. Geophys. Res. Space Physics*, *120*, 9385–9400, doi:10.1002/2015JA021786.

Gao, Z., Z. Su, H. Zhu, F. Xiao, H. Zheng, Y. Wang, C. Shen, and S. Wang (2016), Intense low-frequency chorus waves observed by Van Allen Probes: Fine structures and potential effect on radiation belt electrons, *Geophys. Res. Lett.*, *43*, 967–977, doi:10.1002/2016GL067687.

Gary, S. P. (1993), Theory of Space Plasma Microinstabilities, Cambridge Univ. Press, New York.

Ginzburg (1960), Certain Theoretical Aspects of Radiation Due to Superluminal Motion in a Medium, *Sov. Phys. Usp.* 2 874, https://doi.org/10.1070/PU1960v002n06ABEH003185

Glauert, S. A., and R. B. Horne (2005), Calculation of pitch angle and energy diffusion coefficients with the PADIE code, J. Geophys. Res., 110, A04206, doi:10.1029/2004JA010851.

Glauert, S. A., R. B. Horne, and N. P. Meredith (2014), Three-dimensional electron radiation belt simulations using the BAS Radiation Belt Model with new diffusion models for chorus, plasmaspheric hiss, and lightning-generated whistlers, *J. Geophys. Res. Space Physics*, *119*, 268–289, doi:10.1002/2013JA019281.

Golden, D. I., M. Spasojevic, W. Li, and Y. Nishimura (2012), Statistical modeling of plasmaspheric hiss amplitude using solar wind measurements and geomagnetic indices, Geophys. Res. Lett., 39, L06103, doi:10.1029/ 2012GL051185.

Goldstein, J., S. Kanekal, D. N. Baker, and B. R. Sandel (2005), Dynamic relationship between the outer radiation belt and the plasmapause during March–May 2001, Geophys. Res. Lett., 32, L15104, doi:10.1029/2005GL023431.

Goldstein, J., et al. (2016), The relationship between the plasmapause and outer belt electrons, *J. Geophys. Res. Space Physics*, *121*, doi:10.1002/2016JA023046.

Green, J. C., T. G. Onsager, T. P. O'Brien, and D. N. Baker (2004), Testing loss mechanisms capable of rapidly depleting relativistic electron flux in the Earth's outer radiation belt, *J. Geophys. Res.*, *109*, A12211, doi:10.1029/2004JA010579.[1 SEP]

Greifinger, C., and P. S. Greifinger (1968), Theory of hydromagnetic propagation in the ionosphere waveguide, J. Geophys. Res., 73, 7473–7490, doi:10.1029/JA073i023p07473.

Grison, B., O. Santolk, N. Cornilleau-Wehrlin, A. Masson, M. J. Engebretson, J. S. Pickett, Y. Omura, P. Robert, and R. Nomura (2013), EMIC triggered chorus emissions in Cluster data, J. Geophys. Res. Space Physics, 118, 1159–1169, doi:10.1002/jgra.50178.

Halford, A. J., B. J. Fraser, and S. K. Morley (2010), EMIC wave activity during geomagnetic storm and nonstorm periods: CRRES results, J. Geophys. Res., 115, A12248, doi:10.1029/2010JA015716.

Halford, A. J., B. J. Fraser, and ⬚S. K. Morley (2015a), EMIC waves and plasmaspheric and plume density: CRRES results, *J. Geophys. Res. Space Physics*, *120*, doi:10.1002/2014JA020338. ⬚

Halford, A. J., et al. (2015b), BARREL observations of an ICME-shock impact with the magnetosphere and the resultant radiation belt electron loss, *J. Geophys. Res. Space Physics*, *120*, 2557–2570, doi:10.1002/2014JA020873. ⬚

Haque, N., M. Spasojevic, O. Santolík, and U. S. Inan (2010), Wave normal angles of magnetospheric chorus emissions observed on the Polar spacecraft, J. Geophys. Res., 115, A00F07, doi:10.1029/2009JA014717.

Hartley, D. P., Kletzing, C. A., Santolík, O., Chen, L., & Horne, R. B. (2018). Statistical properties of plasmaspheric hiss from Van Allen Probes observations. *Journal of Geophysical Research: Space Physics*, 123. https://doi.org/10.1002/2017JA024593

Hayakawa, M., Y. Yamanaka, M. Parrot, and F. Lefeuvre (1984), The wave normals of magnetospheric chorus emissions observed on board GEOS 2, J. Geophys. Res., 89(A5), 2811–2821, doi:10.1029/JA089iA05p02811.

He, Y., F. Xiao, Q. Zhou, C. Yang, S. Liu, D. N. Baker, C. A. Kletzing, W. S. Kurth, G. B. Hospodarsky, H. E. Spence, et al. (2015), Van Allen Probes observation and modeling of chorus excitation and propagation during weak geomagnetic activities, J. Geophys. Res. Space Physics, 120, 6371–6385, doi:10.1002/2015JA021376.

He, Z., Q. Yan, Y. Chu, and Y. Cao (2016), Wave-driven gradual loss of energetic electrons in the slot region, *J. Geophys. Res. Space Physics*, *121*, 8614–8623, doi:10.1002/2016JA023087.

Helliwell, R.A. (1965), Whistlers and Related Ionospheric Phenomena, Stanford University Press, Stanford Calif.

Hendry, A. T., C. J. Rodger, and M. A. Clilverd (2017), Evidence of sub-MeV EMIC-driven electron precipitation, *Geophys. Res. Lett.*, *44*, 1210–1218, doi:10.1002/2016GL071807.

Hess, W. N. (1963), The artificial radiation belt made on July 9, 1962, J. Geophys. Res., 68(3), 667–683, doi:10.1029/JZ068i003p00667.

Hikishima, M., Y. Omura, and D. Summers (2010), Microburst precipitation of energetic electrons associated with chorus wave generation, Geophys. Res. Lett., 37, L07103, doi:10.1029/2010GL042678.

Horne, R. B., and R. Thorne (1994), Convective instabilities of electromagnetic ion cyclotron waves in the outer magnetosphere, J. Geophys. Res., 99, 17,259–17,273.

Horne, R.B. & Thorne, R.M. (1998), Potential waves for relativistic electron scattering and stochastic acceleration during magnetic storms, Geophysical Research Letters. 25. 3011-3014.

Horne, R. B., S. A. Glauert, and R. M. Thorne (2003a), Resonant diffusion of radiation belt electrons by whistler-mode chorus, Geophys. Res. Lett., 30(9), 1493, doi:10.1029/2003GL016963.

Horne, R. B., and R. M. Thorne (2003b), Relativistic electron acceleration and precipitation during resonant interactions with whistler-mode chorus, Geophys. Res. Lett., 30(10), 1527, doi:10.1029/2003GL016973.

Horne, R. B., Thorne, R. M., Shprits, Y. Y., Meredith, N.P., Glauert, S.A. (2005), Wave acceleration of electrons in the Van Allen radiation belts, Nature 437, 227–230, doi:10.1038/nature03939.

Horne, R. B., S. A. Glauert, N. P. Meredith, D. Boscher, V. Maget, D. Heynderickx, and D. Pitchford (2013), Space weather impacts on satellites and forecasting the Earth's electron radiation belts with SPACECAST, Space Weather, 11, 169–186, doi:10.1002/swe.20023.

Hsieh, Y.-K, & Omura, Y. (2017). Study of wave-particle interactions for whistler mode waves at oblique angles by utilizing the gyroaveraging method. *Radio Science*, *52*. https://doi.org/10.1002/2017RS006245

Huang, C. Y., C. K. Goertz, and R. R. Anderson (1983), A theoretical study of plasmaspheric hiss generation, J. Geophys. Res., 88(A10), 7927–7940, doi:10.1029/JA088iA10p07927.

Hudson, M.K., B.T. Kress, H-R. Mueller, J.A. Zastrow, and J.B. Blake (2008), Relationship of the Van Allen radiation belts to solar wind drivers, J. Atmos. and Solar-Terr. Phys., 70, 5, https://doi.org/10.1016/j.jastp.2007.11.003

Hudson, M. K., D. N. Baker, J. Goldstein, B. T. Kress, J. Paral, F. R. Toffoletto, and M. Wiltberger (2014), Simulated magnetopause losses and Van Allen Probe flux dropouts, Geophys. Res. Lett., 41, 1113–1118, doi:10.1002/ 2014GL059222.

Hwang, J. A., D.-Y. Lee, L. R. Lyons, A. J. Smith, S. Zou, K. W. Min, K.-H. Kim, Y.-J. Moon, and Y. D. Park (2007), Statistical significance of association between whistler-mode chorus enhancements and enhanced convection periods during high- speed streams, J. Geophys. Res., 112, A09213, doi:10.1029/2007JA012388.

Imhof, W. L., H. D. Voss, J. B. Reagan, D. W. Datlowe, E. E. Gaines, J. Mobilia, and D. S. Evans (1986), Relativistic electron and energetic ion precipitation spikes near the plasmapause, J. Geophys. Res., 91(A3), 3077–3088, doi:10.1029/JA091iA03p03077.

Imhof, W. L., H. D. Voss, J. Mobilia, D. W. Datlowe, and E. E. Gaines (1991), The precipitation of relativistic electrons near the trapping boundary, J. Geophys. Res., 96(A4), 5619–5629, doi:10.1029/90JA02343.

Imhof, W. L., H. D. Voss, J. Mobilia, D. W. Datlowe, E. E. Gaines, J. P. McGlennon, and U. S. Inan (1992), Relativistic electron microbursts, J. Geophys. Res., 97(A9), 13829–13837, doi:10.1029/92JA01138.

Inan, U. S., Chiu, Y. T., Davison, G. T. (1992), Whistler-mode chorus and morningside aurorae, Geophys. Res. Lett., 19, 7, 653-656.

Inan, U. S., M. Golkowski, M. K. Casey, R. C. Moore, W. Peter, P. Kulkarni, P. Kossey, E. Kennedy, S. Meth, and P. Smit (2007), Subionospheric VLF observations of transmitter-induced precipitation of inner radiation belt electrons, Geophys. Res. Lett., 34, L02106, doi:10.1029/2006GL028494.

Jaynes, A. N., et al. (2014), Evolution of relativistic outer belt electrons during an extended quiescent period, *J. Geophys. Res. Space Physics*, *119*, 9558–9566, doi:10.1002/2014JA020125.

Jaynes, A. N., et al. (2015), Source and seed populations for relativistic electrons: Their roles in radiation belt changes, J. Geophys. Res. Space Physics, 120, 7240–7254, doi:10.1002/ 2015JA021234.

Johnstone, A. D., D. M. Walton, R. Liu, and D. A. Hardy (1993), Pitch angle diffusion of low-energy electrons by whistler mode waves, J. Geophys. Res., 98(A4), 5959–5967, doi:10.1029/92JA02376.

Johnston, W. R., and P. C. Anderson (2010), Storm time occurrence of relativistic electron microbursts in relation to the plasmapause, J. Geophys. Res., 115, A02205, doi:10.1029/2009JA014328.

Jordanova, V. K., D. T. Welling, S. G. Zaharia, L. Chen, and R. M. Thorne (2012), Modeling ring current ion and electron dynamics and plasma instabilities during a high-speed stream driven storm, J. Geophys. Res., 117, A00L08, doi:10.1029/ 2011JA017433.

Kasahara, S., et al. (2018), Pulsating aurora from electron scattering by chorus waves, Nature, 554, 337, 10.1038/nature25505.

Katoh, Y., and Y. Omura (2007), Computer simulation of chorus wave generation in the Earth's inner magnetosphere, Geophys. Res. Lett., 34, L03102, doi:10.1029/2006GL028594.

Katoh, Y., and Y. Omura (2013), Effect of the background magnetic field inhomogeneity on generation processes of whistler-mode chorus and broadband hiss-like emissions, J. Geophys. Res. Space Physics, 118, 4189–4198, doi:10.1002/jgra.50395.

Keika, K., K. Takahashi, A. Y. Ukhorskiy, and Y. Miyoshi (2013), Global characteristics of electromagnetic ion cyclotron waves: Occurrence rate and its storm dependence, J. Geophys. Res. Space Physics, 118, doi:10.1002/jgra.50385.

Kellerman, A. C., Y. Y. Shprits, D. Kondrashov, D. Subbotin, R. A. Makarevich, E. Donovan, and T. Nagai (2014), Three-dimensional data assimilation and reanalysis of radiation belt

electrons: Observations of a four-zone structure using five spacecraft and the VERB code, J. Geophys. Res. Space Physics, 119, 8764–8783, doi:10.1002/2014JA020171.

Kellogg, P. J., C. A. Cattell, K. Goetz, S. J. Monson, and L. B. Wilson III (2011), Large amplitude whistlers in the magnetosphere observed with Wind Waves, J. Geophys. Res., 116, A09224, doi:10.1029/2010JA015919.

Kennel, C. F., and H. E. Petschek (1966), Limit on stably trapped particle fluxes, J. Geophys. Res., 71(1), 1–28, doi:10.1029/JZ071i001p00001.

Kersten, K., C. A. Cattell, A. Breneman, K. Goetz, P. J. Kellogg, J. R. Wygant, L. B. Wilson III, J. B. Blake, M. D. Looper, and I. Roth (2011), Observation of relativistic electron microbursts in conjunction with intense radiation belt whistler mode waves, Geophys. Res. Lett., 38, L08107, doi:10.1029/2011GL046810.

Kilpua, E. K. J., H. Hietala, D. L. Turner, H. E. J. Koskinen, T. I. Pulkkinen, J. V. Rodriguez, G. D. Reeves, S. G. Claudepierre, and H. E. Spence (2015), Unraveling the drivers of the storm time radiation belt response, *Geophys. Res. Lett.*, *42*, 3076–3084, doi:10.1002/2015GL063542.

Kim, K.C., Y. Shprits, D. Subbotin, and B. Ni (2011), Understanding the dynamic evolution of the relativistic electron slot region including radial and pitch angle diffusion, J. Geophys. Res., 116, A10214, doi:10.1029/2011JA016684.

Kim, K.C., and Shprits, Yuri (2013), Long-term relativistic radiation belt electron responses to GEM magnetic storms, Journal of Atmospheric and Solar-Terrestrial Physics 100-101 (2013) 59–67

Kletzing, C.A., et al. (2014), Evidence for Significant Local Generation of Plasmaspheric Hiss, American Geophysical Union, Fall Meeting 2014, abstract id.SM14A-09, 2014AGUFMSM14A..09K

Klumpar, D., et al. (2015), Flight system technologies enabling the twin-CubeSat FIREBIRD-II scientific mission, Proceedings of the 29th Annual AIAA/USU Conference on Small Satellites.

Koons, C. H, and McPherson, A. D. (1972). Observation of very-low-frequency whistler-mode waves in the region of the radiation-belt slot. Journal of Geophysical Research. 77. 3475-. 10.1029/JA077i019p03475.

Kozyra, J. U., T. E. Cravens, A. F. Nagy, E. G. Fontheim, and R. S. B. Ong (1984), Effects of energetic heavy ions on electromagnetic ion cyclotron wave generation in the plasmapause region, J. Geophys. Res., 89(A4), 2217–2233, doi:10.1029/JA089iA04p02217.

Laakso, H., O. Santolik, R. Horne, I. Kolmasová, P. Escoubet, A. Masson, and M. Taylor (2015), Identifying the source region of plasmaspheric hiss, Geophys. Res. Lett., 42, 3141–3149, doi:10.1002/2015GL063755.

Lakhina, G. S., B. T. Tsurutani, O. P. Verkhoglyadova, and J. S. Pickett (2010), Pitch angle transport of electrons due to cyclotron interactions with the coherent chorus subelements, J. Geophys. Res., 115, A00F15, doi:10.1029/2009JA014885.

Lam, M. M., R. B. Horne, N. P. Meredith, S. A. Glauert, T. Moffat-Griffin, and J. C. Green (2010), Origin of energetic electron precipitation >30 keV into the atmosphere, J. Geophys. Res., 115, A00F08, doi:10.1029/2009JA014619.

Lampton, M. (1967), Daytime observations of energetic auroral-zone electrons, J. Geophys. Res., 72(23), 5817–5823, doi:10.1029/JZ072i023p05817.

LeDocq, M.J., Gurnett, D.A., and Hospodarsky, G.B. (1998), Chorus source locations from VLF Poynting flux measurements with the Polar spacecraft, Geophys. Res. Lett., DOI: 10.1029/1998GL900071

Lee, J., K. Min, and K.-S. Kim (2013), Characteristic dimension of electromagnetic ion cyclotron wave activity in the magnetosphere, J. Geophys. Res. Space Physics, 118, 1651–1658, doi:10.1002/jgra.50242.

Li, J., et al. (2017), Coherently modulated whistler mode waves simultaneously observed over unexpectedly large spatial scales, J. Geophys. Res. Space Physics, 122, 1871–1882, doi:10.1002/ 2016JA023706.

Li, W., R. M. Thorne, J. Bortnik, Y. Nishimura, V. Angelopoulos, L. Chen, J. P. McFadden, and J. W. Bonnell (2010), Global distributions of suprathermal electrons observed on THEMIS and potential mechanisms for access into the plasmasphere, J. Geophys. Res., 115, A00J10, doi:10.1029/2010JA015687.

Li, W., R. M. Thorne, J. Bortnik, X. Tao, and V. Angelopoulos (2012), Characteristics of hiss-like and discrete whistler-mode emissions, Geophys. Res. Lett., 39, L18106, doi:10.1029/2012GL053206.

Li, W., et al., An unusual enhancement of low-frequency plasmaspheric hiss in the outer plasmasphere associated with substorm-injected electrons (2013a), Geophys. Res. Lett., 40, 3798–3803, doi:10.1002/grl.50787.

Li, W., B. Ni, R. M. Thorne, J. Bortnik, J. C. Green, C. A. Kletzing, W. S. Kurth, and G. B. Hospodarsky (2013b), Constructing the global distribution of chorus wave intensity using measurements of electrons by the POES satellites and waves by the Van Allen Probes, Geophys. Res. Lett., 40, doi:10.1002/grl.50920.

Li, W., et al. (2014), Evidence of stronger pitch angle scattering loss caused by oblique whistler-mode waves as compared with quasi-parallel waves, Geophys. Res. Lett., 41, 6063–6070, doi:10.1002/ 2014GL061260.

Li, W., L. Chen, J. Bortnik, R. M. Thorne, V. Angelopoulos, C. A. Kletzing, W. S. Kurth, and G. B. Hospodarsky (2015a), First evidence for chorus at a large geocentric distance as a source of

plasmaspheric hiss: Coordinated THEMIS and Van Allen Probes observation, Geophys. Res. Lett., 42, 241–248, doi:10.1002/2014GL062832.

Li, W., Q. Ma, R. M. Thorne, J. Bortnik, C. A. Kletzing, W. S. Kurth, G. B. Hospodarsky, and Y. Nishimura (2015b), Statistical properties of plasmaspheric hiss derived from Van Allen Probes data and their effects on radiation belt electron dynamics, J. Geophys. Res. Space Physics, 120, 3393–3405, doi:10.1002/ 2015JA021048. [SEP]

Li, W., R. M. Thorne, J. Bortnik, D. N. Baker, G. D. Reeves, S. G. Kanekal, H. E. Spence, and J. C. Green (2015c), Solar wind conditions leading to efficient radiation belt electron acceleration: A superposed epoch analysis, Geophys. Res. Lett., 42, 6906–6915, doi:10.1002/2015GL065342. [SEP]

Li, W., O. Santolik, J. Bortnik, R. M. Thorne, C. A. Kletzing, W. S. Kurth, and [SEP] G. B. Hospodarsky (2016), New chorus wave properties near the equator from Van Allen Probes wave observations, Geophys. Res. Lett., 43, 4725–4735, doi:10.1002/2016GL068780. [SEP]

Li, X., et al. (1993), Simulation of the prompt energization and transport of radiation belt particles during the March 24, 1991 SSC, Geophys. Res. Lett., DOI: 10.1029/93GL02701

Li, X., D. N. Baker, M. Temerin, T. E. Cayton, E. G. D. Reeves, R. A. Christensen, J. B. Blake, M. D. Looper, R. Nakamura, and S. G. Kanekal (1997), Multisatellite observations of the outer zone electron variation during the November 3 – 4, 1993, magnetic storm, J. Geophys. Res., 102, 14,123 – 14,140.

Li, X., D. N. Baker, T. P. O'Brien, L. Xie, and Q. G. Zong (2006), Correlation between the inner edge of outer radiation belt electrons and the innermost plasmapause location, Geophys. Res. Lett., 33, L14107, doi:10.1029/2006GL026294.

Li, X., A. B. Barker, D. N. Baker, W. C. Tu, T. E. Sarris, R. S. Selesnick, R. Friedel, and C. Shen (2009), Modeling the deep penetration of outer belt electrons during the ''Halloween'' magnetic storm in 2003, Space Weather, 7, S02004, doi:10.1029/2008SW000418.

Li, X., et al. (2013), First results from CSSWE CubeSat: Characteristics of relativistic electrons in the near-Earth environment during the October 2012 magnetic storms, J. Geophys. Res. Space Physics, 118, doi:10.1002/2013JA019342.

Li, X., R. S. Selesnick, D. N. Baker, A. N. Jaynes, S. G. Kanekal, Q. Schiller, L. Blum, J. Fennell, and J. B. Blake (2015), Upper limit on the inner radiation belt MeV electron intensity, *J. Geophys. Res. Space Physics*, *120*, 1215–1228, doi:10.1002/2014JA020777.

Li, X., D. N. Baker, H. Zhao, K. Zhang, A. N. Jaynes, Q. Schiller, S. G. Kanekal, J. B. Blake, and M. Temerin (2017), Radiation belt electron dynamics at low L (<4): Van Allen Probes era versus previous two solar cycles, J. Geophys. Res. Space Physics, 122, doi:10.1002/ 2017JA023924.

Li, Z., R. M. Millan, and M. K. Hudson (2013), Simulation of the energy distribution of relativistic electron precipitation caused by quasi-linear interactions with EMIC waves, J. Geophys. Res. Space Physics, 118, doi:10.1002/2013JA019163.

Li, Z., et al. (2014), Investigation of EMIC wave scattering as the cause for the BARREL 17 January 2013 relativistic electron precipitation event: A quantitative comparison of simulation with observations, Geophys. Res. Lett., 41, 8722–8729, doi:10.1002/2014GL062273.

Liu, K., D. Winske, S. P. Gary, and G. D. Reeves (2012), Relativistic electron scattering by large amplitude electromagnetic ion cyclotron waves: The role of phase bunching and trapping, *J. Geophys. Res., 117,* A06218, doi:10.1029/2011JA017476.

Lorentzen, K. R., J. B. Blake, U. S. Inan, and J. Bortnik (2001a), Observations of relativistic electron microbursts in association with VLF chorus, J. Geophys. Res., 106(A4), 6017–6027, doi:10.1029/2000JA003018.

Lorentzen, K. R., J. B. Blake, U. S. Inan, and J. Bortnik (2001b), Relativistic electron microbursts during the GEM storms, Geophys. Res. Lett., 28(13), 2573–2576, doi:10.1029/2001GL012926.

Loto'aniu, T. M., R. M. Thorne, B. J. Fraser, and D. Summers (2006), Estimating relativistic electron pitch angle scattering rates using properties of the electromagnetic ion cyclotron wave spectrum, J. Geophys. Res., 111, A04220, doi:10.1029/2005JA011452.

Lyons, L. R., R. M. Thorne, and C. F. Kennel (1972), Pitch-angle diffusion of radiation belt electrons within the plasmasphere, J. Geophys. Res., 77(19), 3455–3474, doi:10.1029/JA077i019p03455.

Lyons, L. R., and R. M. Thorne (1973), Equilibrium structure of radiation belt electrons, J. Geophys. Res., 78(13), 2142–2149, doi:10.1029/JA078i013p02142.

Ma, Q., Li, W., Thorne, R. M., Ni, B., Kletzing, C. A., Kurth, W. S., Hospodarsky, G. B., Reeves, G. D., Henderson, M. G., Spence, H. E., Baker, D. N., Blake, J. B., Fennell, J. F., Claudepierre, S. G. and Angelopoulos, V. (2015), Modeling inward diffusion and slow decay of energetic electrons in the Earth's outer radiation belt. Geophys. Res. Lett., 42: 987–995. doi: 10.1002/2014GL062977.

Ma, Q., Li, W., Thorne, R. M., Bortnik, J., Reeves, G. D., Spence, H. E., ... Baker, D. N. (2017a). Diffusive transport of several hundred keV electrons in the Earth's slot region. Journal of Geophysical Research: Space Physics, 122, 10,235–10,246. https://doi.org/10.1002/2017JA024452

Ma, Q., D. Mourenas, W. Li, A. Artemyev, and R. M. Thorne (2017b), VLF waves from ground-based transmitters observed by the Van Allen Probes: Statistical model and effects on plasmaspheric electrons, Geophys. Res. Lett., 44, doi:10.1002/ 2017GL073885.

Ma, Q., Artemyev, A. V., Mourenas, D., Li, W., Thorne, R. M., Kletzing, C. A., ... Wygant, J. (2017c). Very oblique whistler mode propagation in the radiation belts: Effects of hot plasma and Landau damping. *Geophysical Research Letters*, *44*. https://doi.org/10.1002/2017GL075892

Macúšová, E., et al. (2010), Observations of the relationship between frequency sweep rates of chorus wave packets and plasma density, J. Geophys. Res., 115, A12257, doi:10.1029/2010JA015468.

Malaspina, D. M., J. R. Wygant, R. E. Ergun, G. D. Reeves, R. M. Skoug, and B. A. Larsen (2015), Electric field structures and waves at plasma boundaries in the inner magnetosphere, *J. Geophys. Res. Space Physics*, *120*, 4246–4263, doi:10.1002/2015JA021137.

Malaspina, D. M., A. N. Jaynes, C. Boulé, J. Bortnik, S. A. Thaller, R. E. Ergun, C. A. Kletzing, and J. R. Wygant (2016), The Distribution of Plasmaspheric Hiss Wave Power with Respect to Plasmapause Location, *Geophys. Res. Lett.*, *43*, 7878–7886, doi:10.1002/2016GL069982.

Malaspina, D. M., A. N. Jaynes, G. Hospodarsky, J. Bortnik, R. E. Ergun, and J. Wygant (2017), Statistical properties of low-frequency plasmaspheric hiss, *J. Geophys. Res. Space Physics*, *122*, doi:10.1002/2017JA024328.

Mann, I. R., M. E. Usanova, K. Murphy, M. T. Robertson, D. K. Milling, A. Kale, C. Kletzing, J. Wygant, S. Thaller, and T. Raita (2014), Spatial localization and ducting of EMIC waves: Van Allen Probes and ground-based observations, Geophys. Res. Lett., 41, 785–792, doi:10.1002/2013GL058581.

Mann, I. R., et al. (2016a), Explaining the dynamics of the ultra-relativistic third Van Allen radiation belt, Nat. Phys., doi:10.1038/NPHYS3799.

Mann, I. R., and L. G. Ozeke (2016b), How quickly, how deeply, and how strongly can dynamical outer boundary conditions impact Van Allen radiation belt morphology?, J. Geophys. Res. Space Physics, 121, 5553–5558, doi:10.1002/ 2016JA022647.

Matsui, H., K. W. Paulson, R. B. Torbert, H. E. Spence, C. A. Kletzing, W. S. Kurth, R. M. Skoug, B. A. Larsen, and A. W. Breneman (2016), Nonlinearity in chorus waves during a geomagnetic storm on 1 November 2012, *J. Geophys. Res. Space Physics*, *121*, 358–373, doi:10.1002/2015JA021772.

Matsui, H., Torbert, R. B., Spence, H. E., Argall, M. R., Alm, L., Farrugia, C. J., ... Lindqvist, P.-A. (2017). Relativistic electron increase during chorus wave activities on the 6–8 March 2016 geomagnetic storm. *Journal of Geophysical Research: Space Physics*, *122*. https://doi.org/10.1002/2017JA024540

McCollough, J. P., S. R. Elkington, M. E. Usanova, I. R. Mann, D. N. Baker, and Z. C. Kale (2010), Physical mechanisms of compressional EMIC wave growth, J. Geophys. Res., 115, A10214, doi:10.1029/2010JA015393.

Meredith, N. P., R. B. Horne, and R. R. Anderson (2001), Substorm dependence of chorus amplitudes: Implications for the acceleration of electrons to relativistic energies, J. Geophys. Res., 106(A7), 13165–13178, doi:10.1029/2000JA900156.

Meredith, N. P., R. B. Horne, R. H. A. Iles, R. M. Thorne, D. Heynderickx, and R. R. Anderson (2002), Outer zone relativistic electron acceleration associated with substorm-enhanced whistler mode chorus, J. Geophys. Res., 107(A7), doi:10.1029/2001JA900146.

Meredith, N. P., R. B. Horne, R. M. Thorne, and R. R. Anderson (2003a), Favored regions for chorus-driven electron acceleration to relativistic energies in the Earth's outer radiation belt, Geophys. Res. Lett., 30(16), 1871, doi:10.1029/ 2003GL017698.

Meredith, N. P., R. M. Thorne, R. B. Horne, D. Summers, B. J. Fraser, and R. R. Anderson (2003b), Statistical analysis of relativistic electron energies for cyclotron resonance with EMIC waves observed on CRRES, J. Geophys. Res., 108(A6), 1250, doi:10.1029/2002JA009700.

Meredith, N. P., R. B. Horne, R. M. Thorne, D. Summers, and R. R. Anderson (2004), Substorm dependence of plasmaspheric hiss, J. Geophys. Res., 109, A06209, doi:10.1029/2004JA010387.

Meredith, N. P., R. B. Horne, M. A. Clilverd, D. Horsfall, R. M. Thorne, and R. R. Anderson (2006a), Origins of plasmaspheric hiss, J. Geophys. Res., 111, A09217, doi:10.1029/2006JA011707.

Meredith, N. P., R. B. Horne, S. A. Glauert, R. M. Thorne, D. Summers, J. M. Albert, and R. R. Anderson (2006b), Energetic outer zone electron loss timescales during low geomagnetic activity, *J. Geophys. Res.*, *111*, A05212, doi:10.1029/2005JA011516.

Meredith, N. P., R. B. Horne, S. A. Glauert, and R. R. Anderson (2007), Slot region electron loss timescales due to plasmaspheric hiss and lightning-generated whistlers, J. Geophys. Res., 112, A08214, doi:10.1029/2007JA012413.

Meredith, N. P., R. B. Horne, S. A. Glauert, D. N. Baker, S. G. Kanekal, and J. M. Albert (2009), Relativistic electron loss timescales in the slot region, J. Geophys. Res., 114, A03222, doi:10.1029/2008JA013889.

Meredith, N. P., R. B. Horne, W. Li, R. M. Thorne, and A. Sicard-Piet (2014), Global model of low-frequency chorus ($f_{LHR} < f < 0.1\, f_{ce}$) from multiple satellite observations, *Geophys. Res. Lett.*, *41*, 280–286, doi:10.1002/2013GL059050.

Millan, R. M., R. P. Lin, D. M. Smith, K. R. Lorentzen, and M. P. McCarthy (2002), X-ray observations of MeV electron precipitation with a balloon-borne germanium spectrometer, Geophys. Res. Lett., 29(24), 2194, doi:10.1029/2002GL015922.

Millan, R.M., The BARREL Team (2011), Understanding relativistic electron losses with BARREL, Journal of Atmospheric and Solar-Terrestrial Physics 73 (2011) 1425–1434

Millan, R. M., and D. N. Baker (2012), Acceleration of particles to high energies in Earth's radiation belts, *Space Sci. Rev.*, *173*, 103–131, doi:10.1007/s11214-012-9941-x.

Millan, R.M., McCarthy, M.P., Sample, J.G. et al. (2013), The Balloon Array for RBSP Relativistic Electron Losses (BARREL), Space Sci. Rev. (2013) 179: 503. https://doi.org/10.1007/s11214-013-9971-z

Millan, R. M. (2016), Science highlights from the Balloon Array for Radiation belt Electron Losses (BARREL), American Geophysical Union, Fall Meeting 2016, abstract id.SM42A-01, 2016AGUFMSM42A..01M

Min, K., J. Lee, K. Keika, and W. Li (2012), Global distribution of EMIC waves derived from THEMIS observations, J. Geophys. Res., 117, A05219, doi:10.1029/2012JA017515.[1,SEP]

Mironova, I.A., K.L. Aplin, F. Arnold, G.A. Bazilevskaya, R.G. Harrison, A.A. Krivolutsky, K.A. Nicoll, E.V. Rozanov, Esa Turunen, I.G. Usoskin (2015), Energetic Particle Influence on the Earth's Atmosphere, Space Sci. Rev., November 2015, Volume 194, Issue 1–4, pp 1–96

Miyoshi, Y., K. Sakaguchi, K. Shiokawa, D. Evans, J. Albert, M. Connors, and V. Jordanova (2008), Precipitation of radiation belt electrons by EMIC waves, observed from ground and space, Geophys. Res. Lett., 35(23), doi:10.1029/2008GL035727.

Morley, S. K., R. H. W. Friedel, T. E. Cayton, and E. Noveroske (2010), A rapid, global and prolonged electron radiation belt dropout observed with the Global Positioning System constellation, Geophys. Res. Lett., 37, L06102, doi:10.1029/ 2010GL042772.

Mourenas, D., A. V. Artemyev, J.-F. Ripoll, O. V. Agapitov, and V. V. Krasnoselskikh (2012), Timescales for electron quasi-linear diffusion by parallel and oblique lower-band chorus waves, J. Geophys. Res., 117, A06234, doi:10.1029/2012JA017717.

Mourenas, D., A. V. Artemyev, O. V. Agapitov, and V. Krasnoselskikh (2014), Consequences of geomagnetic activity on energization and loss of radiation belt electrons by oblique chorus waves, *J. Geophys. Res. Space Physics*, *119*, 2775–2796, doi:10.1002/2013JA019674.

Mourenas, D., A. V. Artemyev, Q. Ma, O. V. Agapitov, and W. Li (2016), Fast dropouts of multi-MeV electrons due to combined effects of EMIC and whistler mode waves, *Geophys. Res. Lett.*, **43**, 4155–4163, doi:10.1002/2016GL068921.

Moya P.S., V.A. Pinto, D.G. Sibeck, S.G Kanekal, and D.N. Baker (2017), On the effect of geomagnetic storms on relativistic electrons in the outer radiation belt: Van Allen Probes observations, J. Geophys. Res., 122, doi:10.1002/2017JA024735.

Mozer, F.S., Agapitov, O., Krasnoselskikh, V., Lejosne, S., Reeves, G.D., Roth, I. (2014), Direct Observation of Radiation-Belt Electron Acceleration from Electron-Volt Energies to Megavolts by Nonlinear Whistlers, Phys. Rev. Lett., Volume 113, Issue 3, 10.1103/PhysRevLett.113.035001

Mozer, F. S., Agapitov, O. V., Blake, J. B., & Vasko, I. Y. (2018). Simultaneous observations of lower band chorus emissions at the equator and microburst precipitating electrons in the ionosphere. Geophysical Research Letters, 45. https:// doi.org/10.1002/2017GL076120

Murphy, K. R., I. R. Mann, I. J. Rae, D. G. Sibeck, and C. E. J. Watt (2016), Accurately characterizing the importance of wave-particle interactions in radiation belt dynamics: The pitfalls of statistical wave representations, J. Geophys. Res. Space Physics, 121, 7895–7899, doi:10.1002/ 2016JA022618.

Nagano, I., Yagitani, S., Kojima, H., Matsumoto, H. (1996), Analysis of Wave Normal and Poynting Vectors of the Chorus Emissions Observed by GEOTAIL, 48(3), 299-307, https://doi.org/10.5636/jgg.48.299

Nakamura, R., Baker, D.N., Blake, J.B., Kanekal, S., Klecker, B., Hovestadt, D. (1995), Relativistic electron precipitation enhancements near the outer edge of the radiation belt, Geophys. Res. Lett., 22(9), 1129-1132.

Nakamura, R., M. Isowa, Y. Kamide, D. N. Baker, J. B. Blake, and M. Looper (2000), SAMPEX observations of precipitation bursts in the outer radiation belt, J. Geophys. Res., 105(A7), 15875–15885, doi:10.1029/2000JA900018.

Nakamura, S., Y. Omura, and V. Angelopoulos (2016), A statistical study of EMIC rising and falling tone emissions observed by THEMIS, J. Geophys. Res. Space Physics, 121, doi:10.1002/2016JA022353.

Nakamura, S., Y. Omura, S. Machida, M. Shoji, M. Nosé, and V. Angelopoulos (2014), Electromagnetic ion cyclotron rising tone emissions observed by THEMIS probes outside the plasmapause, J. Geophys. Res. Space Physics, 119, 1874–1886, doi:10.1002/2013JA019146.

Němec, F., O. Santolík, M. Parrot, and C. J. Rodger (2010), Relationship between median intensities of electromagnetic emissions in the VLF range and lightning activity, J. Geophys. Res., 115, A08315, doi:10.1029/2010JA015296.

Němec, F., O. Santolík, J. S. Pickett, M. Parrot, and N. Cornilleau-Wehrlin (2013), Quasiperiodic emissions observed by the Cluster spacecraft and their association with ULF magnetic pulsations, J. Geophys. Res. Space Physics, 118, 4210–4220, doi:10.1002/jgra.50406.

Ni, B., J. Bortnik, R. M. Thorne, Q. Ma, and L. Chen (2013), Resonant scattering and resultant pitch angle evolution of relativistic electrons by plasmaspheric hiss, J. Geophys. Res. Space Physics, 118, 7740–7751, doi:10.1002/2013JA019260.

Ni, B., et al. (2014a), Resonant scattering of energetic electrons by unusual low- frequency hiss, Geophys. Res. Lett., 41, 1854–1861, doi:10.1002/2014GL059389.

Ni, B., W. Li, R. M. Thorne, J. Bortnik, J. C. Green, C. A. Kletzing, W. S. Kurth, G. B. Hospodarsky, and M. de Soria-Santacruz Pich (2014b), A novel technique to construct the global

distribution of whistler mode chorus wave intensity using low-altitude POES electron data, J. Geophys. Res. Space Physics, 119, doi:10.1002/2014JA019935.

Ni, B., et al. (2015), Resonant scattering of outer zone relativistic electrons by multiband EMIC waves and resultant electron loss time scales, J. Geophys. Res. Space Physics, 120, 7357–7373, doi:10.1002/2015JA021466.

Nishimura, Y., et al. (2010), Identifying the Driver of Pulsating Aurora, Science 330, 81 (2010), DOI: 10.1126/science.1193186

Nunn D. (1974) A Self-Consistent Theory of Triggered VLF Emissions. In: McCormac B.M. (eds) Magnetospheric Physics. Astrophysics and Space Science Library (A Series of Books on the Recent Developments of Space Science and of General Geophysics and Astrophysics Published in Connection with the Journal Space Science Reviews), vol 44. Springer, Dordrecht

O'Brien, T. P., M. D. Looper, and J. B. Blake (2004), Quantification of relativistic electron microburst losses during the GEM storms, Geophys. Res. Lett., 31, L04802, doi:10.1029/2003GL018621.

O'Brien, T. P., S. G. Claudepierre, J. B. Blake, J. F. Fennell, J. H. Clemmons, J. L. Roeder, H. E. Spence, G. D. Reeves, and D. N. Baker (2014), An empirically observed pitch-angle diffusion eigenmode in the Earth's electron belt near L* = 5.0, Geophys. Res. Lett., 41, doi:10.1002/2013GL058713.

O'Brien, T. P., S. G. Claudepierre, T. B. Guild, J. F. Fennell, D. L. Turner, J. B. Blake, J. H. Clemmons, and J. L. Roeder (2016), Inner zone and slot electron radial diffusion revisited, Geophys. Res. Lett., 43, 7301–7310, doi:10.1002/2016GL069749.

Omura, Y.S., and D. Summers (2004), Computer simulations of relativistic whistler-mode wave–particle interactions, Physics of Plasmas 11, 3530 (2004); https://doi.org/10.1063/1.1757457

Omura, Y., and D. Summers (2006), Dynamics of high-energy electrons interacting with whistler mode chorus emissions in the magnetosphere, J. Geophys. Res., 111, A09222, doi:10.1029/2006JA011600.

Omura, Y., Nunn, D. and Summers, D. (2012) Generation Processes of Whistler Mode Chorus Emissions: Current Status of Nonlinear Wave Growth Theory, in Dynamics of the Earth's Radiation Belts and Inner Magnetosphere (eds D. Summers, I. R. Mann, D. N. Baker and M. Schulz), American Geophysical Union, Washington, D. C.. doi: 10.1029/2012GM001347

Omura, Y., and Q. Zhao (2012), Nonlinear pitch angle scattering of relativistic electrons by EMIC waves in the inner magnetosphere, J. Geophys. Res., 117, A08227, doi:10.1029/2012JA017943.

Omura, Y., and Q. Zhao (2013), Relativistic electron microbursts due to nonlinear pitch angle scattering by EMIC triggered emissions, J. Geophys. Res. Space Physics, 118, doi:10.1002/jgra.50477.

Omura, Y., S. Nakamura, C. A. Kletzing, D. Summers, and M. Hikishima (2015), Nonlinear wave growth theory of coherent hiss emissions in the plasmasphere, *J. Geophys. Res. Space Physics*, *120*, 7642 – 7657, doi:10.1002/2015JA021520.

Orlova, K., M. Spasojevic, and Y. Shprits (2014), Activity-dependent global model of electron loss inside the plasmasphere, Geophys. Res. Lett., 41, 3744–3751, doi:10.1002/2014GL060100.

Orlova, K., Y. Shprits, and M. Spasojevic (2016), New global loss model of energetic and relativistic electrons based on Van Allen Probes measurements, J. Geophys. Res. Space Physics, 121, 1308– 1314, doi:10.1002/2015JA021878.

Parrot, M., Santolik, O., Cornilleau-Wehrlin, N., Maksimovic, M., and Harvey, C.C. (2003), Source location of chorus emissions observed by Cluster, Ann. Geophys., 21, 473-480, 2003

Paulikas, G. A., and J. B. Blake, Effects of the solar wind on magnetospheric dynamics: Energetic electrons at the synchronous orbit (1979), in Quantitative Modeling of Magnetospheric Processes , Geophys. Monogr. Ser., vol. 21, pp. 180–202, AGU, Washington, D. C.

Paulson, K. W., C. W. Smith, M. R. Lessard, M. J. Engebretson, R. B. Torbert, and C. A. Kletzing (2014), In situ observations of Pc1 pearl pulsations by the Van Allen Probes, Geophys. Res. Lett., 41, 1823–1829, doi:10.1002/2013GL059187.

Perraut, S., A. Roux, P. Robert, R. Gendrin, J.-A. Sauvaud, J.-M. Bosqued, G. Kremser, and A. Korth (1982), A systematic study of ULF waves above F_{H+} from GEOS 1 and 2 measurements and their relationships with proton ring distributions, *J. Geophys. Res.*, 87, 6219–6236, doi:10.1029/JA087iA08p06219.

Pham, K. H., Tu, W., & Xiang, Z. (2017). Quantifying the precipitation loss of radiation belt electrons during a rapid dropout event. Journal of Geophysical Research: Space Physics, 122. https://doi. org/10.1002/2017JA024519

Pickett, J. S., et al. (2010), Cluster observations of EMIC triggered emissions in association with Pc1 waves near Earth's plasmapause, Geophys. Res. Lett., 37, L09104, doi:10.1029/2010GL042648.

Posch, J. L., M. J. Engebretson, M. T. Murphy, M. H. Denton, M. R. Lessard, and R. B. Horne (2010), Probing the relationship between electromagnetic ion cyclotron waves and plasmaspheric plumes near geosynchronous orbit, *J. Geophys. Res.*, *115*, A11205, doi:10.1029/2010JA015446.

Reeves, G. D., K. L. McAdams, R. H. W. Friedel, and T. P. O'Brien, Acceleration and loss of relativistic electrons during geomagnetic storms, Geophys. Res. Lett., 30(10), 1529, doi:10.1029/2002GL016513, 2003.

Reeves, G. D., S. K. Morley, R. H. W. Friedel, M. G. Henderson, T. E. Cayton, G. Cunningham, J. B. Blake, R. A. Christensen, and D. Thomsen (2011), On the relationship between relativistic

electron flux and solar wind velocity: Paulikas and Blake revisited, J. Geophys. Res., 116, A02213, doi:10.1029/2010JA015735.

Remya, B., B. T. Tsurutani, R. V. Reddy, G. S. Lakhina, and R. Hajra (2015), Electromagnetic cyclotron waves in the dayside subsolar outer magnetosphere generated by enhanced solar wind pressure: EMIC wave coherency, J. Geophys. Res. Space Physics, 120, 7536–7551, doi:10.1002/2015JA021327.

Riley, P., and J. J. Love (2017), Extreme geomagnetic storms: Probabilistic forecasts and their uncertainties, *Space Weather*, *15*, 53–64, doi:10.1002/2016SW001470.

Ripoll, J.-F., O. Santolík, G. D. Reeves, W. S. Kurth, M. H. Denton, V. Loridan, S. A. Thaller, C. A. Kletzing, and D. L. Turner (2017), Effects of whistler mode hiss waves in March 2013, J. Geophys. Res. Space Physics, 122, doi:10.1002/2017JA024139.

Rodger, C. J., M. A. Clilverd, and R. J. McCormick (2003), Significance of lightning-generated whistlers to inner radiation belt electron lifetimes, J. Geophys. Res., 108, 1462, doi:10.1029/2003JA009906, A12.

Rodger, C. J., M. A. Clilverd, N. R. Thomson, R. J. Gamble, A. Seppälä, E. Turunen, N. P. Meredith, M. Parrot, J.-A. Sauvaud, and J.-J. Berthelier (2007), Radiation belt electron precipitation into the atmosphere: Recovery from a geomagnetic storm, J. Geophys. Res., 112, A11307, doi:10.1029/2007JA012383.

Rodger, C. J., T. Raita, M. A. Clilverd, A. Seppälä, S. Dietrich, N. R. Thomson, and T. Ulich (2008), Observations of relativistic electron precipitation from the radiation belts driven by EMIC waves, *Geophys. Res. Lett.*, *35*, L16106, doi:10.1029/2008GL034804.

Rodger, C. J., et al. (2010), Contrasting the efficiency of radiation belt losses caused by ducted and nonducted whistler-mode waves from ground-based transmitters, *J. Geophys. Res.*, *115*, A12208, doi:10.1029/2010JA015880.

Rodger, C. J., M. A. Clilverd, A. J. Kavanagh, C. E. J. Watt, P. T. Verronen, and T. Raita (2012), Contrasting the responses of three different ground-based instruments to energetic electron precipitation, Radio Sci., 47, RS2021, doi:10.1029/2011RS004971.

Rodger, C. J., K. Cresswell-Moorcock, and M. A. Clilverd (2016), Nature's Grand Experiment: Linkage between magnetospheric convection and the radiation belts, J. Geophys. Res. Space Physics, 121, 171–189, doi:10.1002/ 2015JA021537.

Rodger, C. J., A. T. Hendry, M. A. Clilverd, C. A. Kletzing, J. B. Brundell, and G. D. Reeves (2015), High-resolution in situ observations of electron precipitation- causing EMIC waves, Geophys. Res. Lett., 42, 9633–9641, doi:10.1002/ 2015GL066581.

Rosenberg, T. J., R. A. Helliwell, and J. P. Katsufrakis (1971), Electron precipitation associated with discrete very-low-frequency emissions, J. Geophys. Res., 76(34), 8445–8452, doi:10.1029/JA076i034p08445.

Rosenberg, T. J., J. C. Siren, D. L. Matthews, K. Marthinsen, J. A. Holtet, A. Egeland, D. L. Carpenter, and R. A. Helliwell (1981), Conjugacy of electron microbursts and VLF chorus, J. Geophys. Res., 86(A7), 5819–5832, doi:10.1029/JA086iA07p05819.

Rosenberg, T. J., R. Wei, D. L. Detrick, and U. S. Inan (1990), Observations and modeling of wave-induced microburst electron precipitation, J. Geophys. Res., 95(A5), 6467–6475, doi:10.1029/JA095iA05p06467.

Roth, I., Temerin, M., Hudson, M. K. (1999), Resonant enhancement of relativistic electron fluxes during geomagnetically active periods. Annales Geophysicae, European Geosciences Union, 17 (5), pp.631-638

Russell, C.T., McPherron, R.L. & Coleman (1972), Fluctuating Magnetic Fields in the Magnetosphere. I: ELF and VLF Fluctuations, P.J. Space Sci Rev, 12: 810. https://doi.org/10.1007/BF00173072

Russell, C. T., J. G. Luhmann, and L. K. Jian (2010), How unprecedented a solar minimum?, Rev. Geophys., 48, RG2004, doi:10.1029/2009RG000316.

Saikin, A. A., J.-C. Zhang, R. C. Allen, C. W. Smith, L. M. Kistler, H. E. Spence, R. B. Torbert, C. A. Kletzing, and V. K. Jordanova (2015), The occurrence and wave properties of H+-, He+-, and O+-band EMIC waves observed by the Van Allen Probes, J. Geophys. Res. Space Physics, 120, doi:10.1002/2015JA021358.

Saito, S., Y. Miyoshi, and K. Seki (2012), Relativistic electron microbursts associated with whistler chorus rising tone elements: GEMSIS-RBW simulations, J. Geophys. Res., 117, A10206, doi:10.1029/2012JA018020.

Sandanger, M., F. Søraas, K. Aarsnes, K. Oksavik, and D. S. Evans (2007), Loss of relativistic electrons: Evidence for pitch angle scattering by electromagnetic ion cyclotron waves excited by unstable ring current protons, J. Geophys. Res., 112(A12), doi:10.1029/2006JA012138.

Sandel, B.R., Goldstein, J., Gallagher, D.L., Spasojevic, M. (2003), Extreme Ultraviolet Imager Observations of the Structure and Dynamics of the Plasmasphere, Space Science Reviews, Vol. 109, issue 1-4, pp 25-46

Santolík, O., and D. Gurnett (2003), Transverse dimensions of chorus in the source region, Geophys. Res. Lett., 30(2), 1031, doi:10.1029/ 2002GL016178.

Santolík, O., D. A. Gurnett, and J. S. Pickett (2004a), Multipoint investigation of the source region of storm-time chorus, Ann. Geophys., 22, 2555–2563.

Santolık, O., D. A. Gurnett, J. S. Pickett, M. Parrot, and N. Cornilleau-Wehrlin (2004b), A microscopic and nanoscopic view of storm-time chorus on 31 March 2001, Geophys. Res. Lett., 31, L02801, doi:10.1029/2003GL018757.

Santolik, O., D.A. Gurnett, J.S. Pickett, M. Parrot, N. Cornilleau-Wehrlin (2005), Central position of the source region of storm-time chorus, Planetary and Space Sci., ISSN: 0032-0633, Vol: 53, Issue: 1, Page: 299-305

Santolík, O., J. S. Pickett, D. A. Gurnett, J. D. Menietti, B. T. Tsurutani, and O. Verkhoglyadova (2010), Survey of Poynting flux of whistler mode chorus in the outer zone, J. Geophys. Res., 115, A00F13, doi:10.1029/2009JA014925.

Santolík, O., C. A. Kletzing, W. S. Kurth, G. B. Hospodarsky, and S. R. Bounds (2014a), Fine structure of large-amplitude chorus wave packets, Geophys. Res. Lett., 41, doi:10.1002/2013GL058889

Santolík, O., E. Macúšová, I. Kolmašová, N. Cornilleau-Wehrlin, and Y. de Conchy (2014b), Propagation of lower-band whistler-mode waves in the outer Van Allen belt: Systematic analysis of⎵11 years of multi-component data from the Cluster spacecraft, Geophys. Res. Lett., 41, 2729–2737, doi:10.1002/ 2014GL059815.⎵

Sazhin, S. S., and M. Hayakawa (1992), Magnetospheric chorus emissions—A review, *Planet. Space Sci.*, *40*, 681–697, doi:10.1016/0032-0633(92)90009-D.

Schiller, Q., W. Tu, A. F. Ali, X. Li,⎵H. C. Godinez, D. L. Turner, S. K. Morley, and M. G. Henderson (2017), Simultaneous event-specific estimates of transport, loss, and source rates ⎵for relativistic outer radiation belt electrons, J. Geophys. Res. Space Physics, 122, 3354–3373, doi:10.1002/ 2016JA023093.

Selesnick, R. S., J. B. Blake, and R. A. Mewaldt (2003), Atmospheric losses of radiation belt electrons, J. Geophys. Res., 108, 1468, doi:10.1029/2003JA010160, A12.

SenGupta A., C.A. Kletzing, R. Howk, W.S Kurth, and M. Matheny(2017), Automated Identification and Shape Analysis of Chorus Elements in the Van Allen Radiation Belts, J. Geophys. Res., 122, doi:10.1002/2017JA023949.

Shekhar, S., Millan, R., & Smith, D. (2017). A statistical study of the spatial extent of relativistic electron precipitation with polar orbiting environmental satellites. Journal of Geophysical Research: Space Physics, 122, 11,274–11,284. https://doi.org/10.1002/2017JA024716

Shi, R., Li, W., Ma, Q., Reeves, G. D., Kletzing, C. A., Kurth, W. S., ... Claudepierre, S. G. (2017). Systematic evaluation of low-frequency hiss and energetic electron injections. Journal of Geophysical Research: Space Physics, 122. https://doi.org/10.1002/2017JA024571

Shklyar, D. & Matsumoto, H. Surv Geophys (2009) 30: 55. https://doi.org/10.1007/s10712-009-9061-7

Shoji, M., and Y. Omura (2013), Triggering process of electromagnetic ion cyclotron rising tone emissions in the inner magnetosphere, J. Geophys. Res. Space Physics, 118, 5553–5561, doi:10.1002/jgra.50523.⎵

Shprits, Y. Y., R. M. Thorne, R. Friedel, G. D. Reeves, J. Fennell, D. N. Baker, and S. G. Kanekal (2006), Outward radial diffusion driven by losses at magnetopause, J. Geophys. Res., 111, A11214, doi:10.1029/2006JA011657.

Shprits, Y. Y., N. P. Meredith, and R. M. Thorne (2007), Parameterization of radiation belt electron loss timescales due to interactions with chorus waves, Geophys. Res. Lett., 34, L11110, doi:10.1029/2006GL029050.

Shprits, Y. Y., D. Subbotin, and B. Ni (2009), Evolution of electron fluxes in the outer radiation belt computed with the VERB code, J. Geophys. Res., 114, A11209, doi:10.1029/2008JA013784.

Shprits, Y. Y., D. Subbotin, A. Drozdov, M. E. Usanova, A. Kellerman, K. Orlova, D. N. Baker, D. L. Turner, and K.-C. Kim (2013), Unusual stable trapping of the ultra-relativistic electrons in the Van Allen radiation belts, Nat. Phys., doi:10.1038/nphys2760.

Sigsbee, K., et al. (2016), Van Allen Probes, THEMIS, GOES, and Cluster observations of EMIC waves, ULF pulsations, and an electron flux dropout, J. Geophys. Res. Space Physics, 121, 1990–2008, doi:10.1002/2014JA020877.

Silin, I., I. R. Mann, R. D. Sydora, D. Summers, and R. L. Mace (2011), Warm plasma effects on electromagnetic ion cyclotron wave MeV electron interactions in the magnetosphere, *J. Geophys. Res., 116,* A05215, doi:10.1029/2010JA016398.

Sivadas, N., Semeter, J., Nishimura, Y., & Kero, A. (2017). Simultaneous measurements of substorm-related electron energization in the ionosphere and the plasma sheet. Journal of Geophysical Research: Space Physics, 122. https//doi. org/10.1002/2017JA023995

Shprits, Y. Y., and B. Ni (2009), Dependence of the quasi-linear scattering rates on the wave normal distribution of chorus waves, J. Geophys. Res., 114, A11205, doi:10.1029/2009JA014223.

Shprits, Y. Y., A. Kellerman, N. Aseev, A. Y. Drozdov, and I. Michaelis (2017), Multi-MeV electron loss in the heart of the radiation belts, Geophys. Res. Lett., 44, 1204–1209, doi:10.1002/2016GL072258.

Smith, D. M., E. P. Casavant, M. D. Comess, X. Liang, G. S. Bowers, R. S. Selesnick, L. B. N.Clausen, R. M. Millan, and J. G. Sample (2016), The causes of the hardest electron precipitation events seen with SAMPEX, *J. Geophys. Res. Space Physics*, *121*, doi:10.1002/2016JA022346.

de Soria-Santacruz, M., M. Spasojevic, and L. Chen (2013), EMIC waves growth and guiding in the presence of cold plasma density irregularities, Geophys. Res. Lett., 40, doi:10.1002/grl.50484.

Sonwalkar, V. S., and U. S. Inan (1989), Lightning as an embryonic source of VLF hiss, J. Geophys. Res., 94(A6), 6986–6994, doi:10.1029/JA094iA06p06986.

Spasojevic, M., and Y. Y. Shprits (2013), Chorus functional dependencies derived from CRRES data, Geophys. Res. Lett., 40, 3793–3797, doi:10.1002/grl.50755.

Spasojevic, M., M. F. Thomsen, P. J. Chi, and B. R. Sandel (2005), Afternoon subauroral proton precipitation resulting from ring current – plasmasphere interaction, in Inner Magnetosphere Interactions: New Perspectives From Imaging, Geophys. Monogr. Ser., vol. 159, edited by J. Burch, M. Schulz, and H. Spence, pp. 85–99, AGU, Washington, D. C.

Stix, T. H. (1992), Waves in plasmas, New York: American Institute of Physics

Storey, L.R.O. (1953), An investigation of whistling atmospherics, DOI: 10.1098/rsta.1953.0011

Su, Z., et al. (2014), Intense duskside lower band chorus waves observed by Van Allen Probes: Generation and potential acceleration effect on radiation belt electrons, *J. Geophys. Res. Space Physics*, *119*, 4266–4273, doi:10.1002/2014JA019919.

Su, Z., Liu, N., Zheng, H., Wang, Y., & Wang, S. (2018). Large-amplitude extremely low frequency hiss waves in plasmaspheric plumes. Geophysical Research Letters, 45. https://doi.org/10.1002/2017GL076754

Subbotin, D. A., Y. Y. Shprits, and B. Ni (2011), Long-term radiation belt simulation with the VERB 3-D code: Comparison with CRRES observations, J. Geophys. Res., 116, A12210, doi:10.1029/2011JA017019.

Summers, D., R. M. Thorne, and F. Xiao (1998), Relativistic theory of wave-particle resonant diffusion with application to electron acceleration in the magnetosphere, J. Geophys. Res., 103(A9), 20487–20500, doi:10.1029/98JA01740.

Summers, D., and R. M. Thorne (2003), Relativistic electron pitch-angle scattering by electromagnetic ion cyclotron waves during geomagnetic storms, J. Geophys. Res., 108(A4), 1143, doi:10.1029/2002JA009489.

Summers, D., B. Ni, N. P. Meredith, R. B. Horne, R. M. Thorne, M. B. Moldwin, and R. R. Anderson (2008), Electron scattering by whistler-mode ELF hiss in plasmaspheric plumes, J. Geophys. Res., 113, A04219, doi:10.1029/2007JA012678.

Summers, D., R. Tang, and R. M. Thorne (2009), Limit on stably trapped particle fluxes in planetary magnetospheres, J. Geophys. Res., 114, A10210, doi:10.1029/2009JA014428.

Summers, D., Y. Omura, S. Nakamura, and C. A. Kletzing (2014), Fine structure of plasmaspheric hiss, *J. Geophys. Res. Space Physics*, *119*, 9134–9149, doi:10.1002/2014JA020437.

Tao, X., J. Bortnik, J. M. Albert, and R. M. Thorne (2012), Comparison of bounce-averaged quasi-linear diffusion coefficients for parallel propagating whistler mode waves with test particle simulations, J. Geophys. Res., 117, A10205, doi:10.1029/2012JA017931.

Taubenschuss, U., Y. V. Khotyaintsev, O. Santolík, A. Vaivads, C. M. Cully, O. Le Contel, and V. Angelopoulos (2014), Wave normal angles of whistler mode chorus rising and falling tones, *J. Geophys. Res. Space Physics*, *119*, 9567–9578, doi:10.1002/2014JA020575.

Teng, S., Tao, X., Xie, Y., Zonca, F., Chen, L., Fang, W. B., & Wang, S. (2017). Analysis of the duration of rising tone chorus elements. *Geophysical Research Letters*, *44*. https://doi.org/10.1002/2017GL075824

Thorne, R. M., et al. (2013), Evolution and slow decay of an unusual narrow ring of relativistic electrons near L ~ 3.2 following the September 2012 magnetic storm, Geophys. Res. Lett., 40, doi:10.1002/grl.50627.

Thorne, R. M., E. J. Smith, R. K. Burton, and R. E. Holzer (1973), Plasmaspheric hiss, J. Geophys. Res., 78(10), 1581–1596, doi:10.1029/JA078i010p01581.

Thorne, R., S. Church, and D. Gorney (1979), On the origin of plasmaspheric hiss: The importance of wave propagation and the plasmapause, J. Geophys. Res., 84(A9), 5241–5247, doi:10.1029/JA084iA09p05241.

Thorne, R. M., Horne, R. B., Glauert, S., Meredith, N. P., Shprits, Y. Y., Summers, D. and Anderson, R. R. (2005) The Influence of Wave-Particle Interactions on Relativistic Electron Dynamics During Storms, in Inner Magnetosphere Interactions: New Perspectives from Imaging (eds J. Burch, M. Schulz and H. Spence), American Geophysical Union, Washington, D. C.. doi: 10.1029/159GM07

Thorne, R. M., Radiation belt dynamics: The importance of wave particle interactions (2010), Geophys. Res. Lett., 37, L22107, doi:10.1029/2010GL044990.

Thorne, R. M., Ni, B., Tao, X., Horne, R. B., Meredith, N. P. (2010), Scattering by chorus waves as the dominant cause of diffuse auroral precipitation, Nature 467, 943-946, doi: 10.1038/nature09467

Thorne, R.M. et al. (2013), Rapid local acceleration of relativistic radiation-belt electrons by magnetospheric chorus, N*ature* 504, 411–414 (19 December 2013), doi:10.1038/nature12889

Thorne, R. M., and C. F. Kennel, Relativistic electron precipitation during magnetic storm main phase, J. Geophys. Res., 76, 4446, 1971.

Titova, E. E., B. V. Kozelov, A. G. Demekhov, J. Manninen, O. Santolik, C. A. Kletzing, and G. Reeves (2015), Identification of the source of quasiperiodic VLF emissions using ground-based and Van Allen Probes satellite observations, Geophys. Res. Lett., 42, 6137–6145, doi:10.1002/2015GL064911.

Tsintsadze, N. L., T. D. Kaladze, J. W. Van Dam, W. Horton, X. R. Fu, and T. W. Garner (2010), Nonlinear dynamics of the electromagnetic ion cyclotron structures in the inner magnetosphere, J. Geophys. Res., 115, A07204, doi:10.1029/2009JA014555.

Tsurutani, B. T., and E. J. Smith (1974), Postmidnight chorus: A substorm phenomenon, J. Geophys. Res., 79(1), 118–127, doi:10.1029/JA079i001p00118.

Tsurutani, B. T., and E. J. Smith (1977), Two types of magnetospheric ELF chorus and their substorm dependences, J. Geophys. Res., 82(32), 5112–5128, doi:10.1029/JA082i032p05112.

Tsurutani, B. T., O. P. Verkhoglyadova, G. S. Lakhina, and S. Yagitani (2009), Properties of dayside outer zone chorus during HILDCAA events: Loss of energetic electrons, J. Geophys. Res., 114, A03207, doi:10.1029/2008JA013353.

Tsurutani, B. T., B. J. Falkowski, O. P. Verkhoglyadova, J. S. Pickett, O. Santolík, and G. S. Lakhina (2012), Dayside ELF electromagnetic wave survey: A Polar statistical study of chorus and hiss, J. Geophys. Res., 117, A00L12, doi:10.1029/2011JA017180.

Tsurutani, B. T., B. J. Falkowski, J. S. Pickett, O. Santolik, and G. S. Lakhina (2015), Plasmaspheric hiss properties: Observations from Polar, J. Geophys. Res. Space Physics, 120, doi:10.1002/ 2014JA020518.

Tu, W., G. S. Cunningham, Y. Chen, M. G. Henderson, E. Camporeale, and G. D. Reeves (2013), Modeling radiation belt electron dynamics during GEM challenge intervals with the DREAM3D diffusion model, J. Geophys. Res. Space Physics, 118, 6197–6211, doi:10.1002/jgra.50560.

Tu, W., G. S. Cunningham, Y. Chen, S. K. Morley, G. D. Reeves, J. B. Blake, D. N. Baker, and H. Spence (2014), Event- specific chorus wave and electron seed population models in DREAM3D using the Van Allen Probes, Geophys. Res. Lett., 41, 1359–1366, doi:10.1002/ 2013GL058819.

Turner, D.L., Shprits, Y.Y., Hartinger, M., and Angelopoulos, V. (2012), Explaining sudden losses of outer radiation belt electrons during geomagnetic storms, Nature Physics 8, 208–212, doi:10.1038/nphys2185

Turner, D. L., et al. (2014), On the cause and extent of outer radiation belt losses during the 30 September 2012 dropout event, J. Geophys. Res. Space Physics, 119, doi:10.1002/2013JA019446.

Turner, D. L., T. P. O'Brien, J. F. Fennell, S. G. Claudepierre, J. B. Blake, E. K. J. Kilpua, and H. Hietala (2015), The effects of geomagnetic storms on electrons in Earth's radiation belts, Geophys. Res. Lett., 42, 9176–9184, doi:10.1002/ 2015GL064747.

Turner, D. L., Lee, J. H., Claudepierre, S. G., Fennell, J. F., Blake, J. B., Jaynes, A. N., ... Santolik, O. (2017). Examining coherency scales, substructure, and propagation of whistler mode chorus elements with Magnetospheric Multiscale (MMS). Journal of Geophysical Research: Space Physics, 122. https://doi.org/10.1002/ 2017JA024474

Ukhorskiy, A. Y., M. I. Sitnov, R. M. Millan, B. T. Kress, J. F. Fennell, S. G. Claudepierre, and R. J. Barnes (2015), Global storm time depletion of the outer electron belt, *J. Geophys. Res. Space Physics*, *120*, 2543–2556, doi:10.1002/2014JA020645.

Ukhorskiy, A. Y., Y. Y. Shprits, B. J. Anderson, K. Takahashi, and R. M. Thorne (2010), Rapid scattering of radiation belt electrons by storm-time EMIC waves, Geophys. Res. Lett., 37, L09101, doi:10.1029/2010GL042906.

Usanova, M. E., I. R. Mann, J. Bortnik, L. Shao, and V. Angelopoulos (2012), THEMIS observations of electromagnetic ion cyclotron wave occurrence: Dependence on AE, SYMH, and solar wind dynamic pressure, J. Geophys. Res., 117, A10218, doi:10.1029/2012JA018049.

Usanova, M. E., F. Darrouzet, I. R. Mann, and J. Bortnik (2013), Statistical analysis of EMIC waves in plasmaspheric plumes from Cluster observations, *J. Geophys. Res. Space Physics*, *118*(8), 4946–4951, doi:10.1002/jgra.50464.

Usanova, M. E., D. M. Malaspina, A. N. Jaynes, R. J. Bruder, I. R. Mann, J. R. Wygant, and R. E. Ergun (2016), Van Allen Probes observations of oxygen cyclotron harmonic waves in the inner magnetosphere, Geophys. Res. Lett., 43, 8827–8834, doi:10.1002/2016GL070233.

Vampola, A. L., H. C. Koons, and D. A. McPherson (1971), Outer-zone electron precipitation, J. Geophys. Res., 76(31), 7609–7617, doi:10.1029/JA076i031p07609.

Van Allen, J. A. (1959), The geomagnetically trapped corpuscular radiation, J. Geophys. Res., 64(11), 1683–1689, doi:10.1029/JZ064i011p01683.

Villalón, E., and W. J. Burke (1995), Pitch angle scattering of diffuse auroral electrons by whistler mode waves, J. Geophys. Res., 100(A10), 19361–19369, doi:10.1029/95JA01161.

Walt, M.: Introduction to geomagnetically trapped radiation, Cambridge University Press, Cambridge, 1994.

Wang, D., et al. (2015), Statistical characteristics of EMIC waves: Van Allen Probe observations, J. Geophys. Res. Space Physics, 120, 4400–4408, doi:10.1002/2015JA021089.

Watt, C. E. J., I. J. Rae, K. R. Murphy, C. Anekallu, S. N. Bentley, and C. Forsyth (2017), The parameterization of wave-particle interactions in the Outer Radiation Belt, J. Geophys. Res. Space Physics, 122, doi:10.1002/2017JA024339.

Wilson, L. B., III, C. A. Cattell, P. J. Kellogg, J. R. Wygant, K. Goetz, A. Breneman, and K. Kersten (2011), The properties of large amplitude whistler mode waves in the magnetosphere: Propagation and relationship with geomagnetic activity, Geophys. Res. Lett., 38, L17107, doi:10.1029/2011GL048671.

Winckler, J.R et al. (1962), A study of the precipitation of energetic electrons from the geomagnetic field during magnetic storms, J. Geophys. Res., 67(10), 3717-3736, doi:10.1029/JZ067i010p03717.

Woodger, L. A., A. J. Halford, R. M. Millan, M. P. McCarthy, D. M. Smith, G. S. Bowers, J. G. Sample, B. R. Anderson, and X. Liang (2015), A summary of the BARREL campaigns: Technique for studying electron precipitation. J. Geophys. Res. Space Physics, 120, 4922–4935. doi: 10.1002/2014JA020874.

Wrenn, G. L. & Smith, R. J. K. (1996), The ESD Threat to GEO Satellites: Empirical Models for Observed Effects Due to Both Surface and Internal Charging, Environment Modelling for Space-based Applications, Symposium Proceedings (ESA SP-392). ESTEC Noordwijk, 18-20 September 1996. Editors: W. Burke and T.-D. Guyenne, p.121, 1996ESASP.392..121W

Xiang, Z., Tu, W., Li, X., Ni, B., Morley, S. K., & Baker, D. N. (2017). Understanding the mechanisms of radiation belt dropouts observed by Van Allen Probes. Journal of Geophysical Research: Space Physics, 122, 9858–9879. https://doi.org/ 10.1002/2017JA024487

Xiao, F., et al. (2013), Wave-driven butterfly distribution of Van Allen belt relativistic electrons, Nature Comm., doi:10.1038/ncomms9590.

Xiao, F., et al. (2014), Chorus acceleration of radiation belt relativistic electrons during March 2013 geomagnetic storm, *J. Geophys. Res. Space Physics*, *119*, 3325–3332, doi:10.1002/2014JA019822.

Xiao, F., et al. (2017), Generation of extremely low frequency chorus in Van Allen radiation belts, *J. Geophys. Res. Space Physics*, *122*, 3201–3211, doi:10.1002/2016JA023561.

Yahnin, A. G., T. A. Yahnina, N. V. Semenova, B. B. Gvozdevsky, and A. B. Pashin (2016), Relativistic electron precipitation as seen by NOAA POES, J. Geophys. Res. Space Physics, 121, doi:10.1002/2016JA022765.

Yu, J., L. Y. Li, J. B. Cao, Z. G. Yuan, G. D. Reeves, D. N. Baker, J. B. Blake, and H. Spence (2015), Multiple loss processes of relativistic electrons outside the heart of outer radiation belt during a storm sudden commencement, J. Geophys. Res. Space Physics, 120, 10,275–10,288, doi:10.1002/2015JA021460.

Yu, J., L. Y. Li, J. B. Cao, L. Chen, J. Wang, and J. Yang (2017), Propagation characteristics of plasmaspheric hiss: Van Allen Probe observations and global empirical models, J. Geophys. Res. Space Physics, 122, 4156–4167, doi:10.1002/ 2016JA023372. SEP

Yu, X., Z. Yuan, S. Huang, D. Wang, H. Li, Z. Qiao, and F. Yao (2017), EMIC waves covering wide L shells: MMS and Van Allen Probes observations, J. Geophys. Res. Space Physics, 122, 7387–7395, doi:10.1002/2017JA023982.

Yuan, C., and Q. Zong (2013), The double-belt outer radiation belt during CME- and CIR-driven geomagnetic storms, *J. Geophys. Res. Space Physics*, **118**, 6291–6301, doi:10.1002/jgra.50564.

Yue, C., X. An, J. Bortnik, Q. Ma, W. Li, R. M. Thorne, G. D. Reeves, M. Gkioulidou, D. G. Mitchell, and C. A. Kletzing (2016), The relationship between the macroscopic state of electrons and the properties of chorus waves observed by the Van Allen Probes, *Geophys. Res. Lett.*, *43*, 7804–7812, doi:10.1002/2016GL070084.

Yue, C. Chen, L. Bortnik, J. Ma, Q. Thorne, R. M. Angelopoulos, V., ... Spence, H. E. (2017). The characteristic response of whistler mode waves to interplanetary shocks. Journal of Geophysical Research: Space Physics, 122, 10,047–10,057. https://doi.org/10.1002/2017JA024574

Zhao, H., and X. Li (2013), Modeling energetic electron penetration into the slot region and inner radiation belt, J. Geophys. Res. Space Physics, 118, 6936–6945, doi:10.1002/2013JA019240.

Zhang, X.-J., D. Mourenas, A. V. Artemyev, V. Angelopoulos, and R. M. Thorne (2017), Contemporaneous EMIC and whistler mode waves: Observations and consequences for MeV electron loss, Geophys. Res. Lett., 44, 8113–8121, doi:10.1002/2017GL073886.

Zhima, Z., Chen, L., Xiong, Y., Cao, J. & Fu, H. (2017). On the origin of ionospheric hiss: a conjugate observation. Journal of Geophysical Research: Space Physics, 122. https://doi.org/10.1002/2017JA024803

Zhu, H., et al. (2015), Plasmatrough exohiss waves observed by Van Allen Probes: Evidence for leakage from plasmasphere and resonant scattering of radiation belt electrons, *Geophys. Res. Lett.*, *42*, 1012–1019, doi:10.1002/2014GL062964. [SEP]